Extracellular Sodium Interacts with the HERG Channel at an Outer Pore Site

Franklin M. Mullins,[1] Svetlana Z. Stepanovic,[2] Reshma R. Desai,[1] Alfred L. George, Jr.,[1,3] and Jeffrey R. Balser[1,2]

[1]Department of Pharmacology, [2]Department of Anesthesiology, and [3]Department of Medicine,
Vanderbilt University School of Medicine, Nashville, TN 37232

ABSTRACT Most voltage-gated K^+ currents are relatively insensitive to extracellular Na^+ (Na^+_o), but Na^+_o potently inhibits outward human ether-a-go-go–related gene (HERG)–encoded K^+ channel current (Numaguchi, H., J.P. Johnson, Jr., C.I. Petersen, and J.R. Balser. 2000. *Nat. Neurosci.* 3:429–30). We studied wild-type (WT) and mutant HERG currents and used two strategic probes, intracellular Na^+ (Na^+_i) and extracellular Ba^{2+} (Ba^{2+}_o), to define a site where Na^+_o interacts with HERG. Currents were recorded from transfected Chinese hamster ovary (CHO-K1) cells using the whole-cell voltage clamp technique. Inhibition of WT HERG by Na^+_o was not strongly dependent on the voltage during activating pulses. Three point mutants in the P-loop region (S624A, S624T, S631A) with intact K^+ selectivity and impaired inactivation each had reduced sensitivity to inhibition by Na^+_o. Quantitatively similar effects of Na^+_i to inhibit HERG current were seen in the WT and S624A channels. As S624A has impaired Na^+_o sensitivity, this result suggested that Na^+_o and Na^+_i act at different sites. Extracellular Ba^{2+} (Ba^{2+}_o) blocks K^+ channel pores, and thereby serves as a useful probe of K^+ channel structure. HERG channel inactivation promotes relief of Ba^{2+} block (Weerapura, M., S. Nattel, M. Courtemanche, D. Doern, N. Ethier, and T. Hebert. 2000. *J. Physiol.* 526:265–278). We used this feature of HERG inactivation to distinguish between simple allosteric and pore-occluding models of Na^+_o action. A remote allosteric model predicts that Na^+_o will speed relief of Ba^{2+}_o block by promoting inactivation. Instead, Na^+_o slowed Ba^{2+} egress and Ba^{2+} relieved Na^+_o inhibition, consistent with Na^+_o binding to an outer pore site. The apparent affinities of the outer pore for Na^+_o and K^+_o as measured by slowing of Ba^{2+} egress were compatible with competition between the two ions for the channel pore in their physiological concentration ranges. We also examined the role of the HERG closed state in Na^+_o inhibition. Na^+_o inhibition was inversely related to pulsing frequency in the WT channel, but not in the pore mutant S624A.

KEY WORDS: human ether-a-go-go-related gene • potassium ion channel • ion channel gating • sodium • barium

INTRODUCTION

The human cardiac delayed rectifier K^+ current I_{Kr} is carried by a channel encoded by the human ether-a-go-go–related gene (HERG),* (Sanguinetti et al., 1995). Suppression of I_{Kr} by loss of function mutations in the HERG gene (Curran et al., 1995; Roden and Balser, 1999) or by untoward drug block (Monahan et al., 1990; Roy et al., 1996; Rampe et al., 1997) can prolong the QT interval and predispose patients to the potentially lethal arrhythmia *torsades de pointes*. Studies of I_{Kr} and HERG have begun to illuminate the mechanisms of recognized risk factors for acquired (drug-induced) long QT syndrome, including hypokalemia

(Roden, 1998). Lowering the extracellular potassium concentration ($[K^+]_o$) decreases the magnitude of I_{Kr} (Sanguinetti and Jurkiewicz, 1992) and of outward HERG K^+ currents (Sanguinetti et al., 1995). Further, raising serum $[K^+]$ to the high normal range can normalize QT prolongation in some congenital long QT patients with HERG mutations (Compton et al., 1996) and in patients with acquired QT prolongation (Choy et al., 1997). These effects are "paradoxical" or "anti-Nernstian" in that their direction opposes that predicted by the simple change in electrochemical driving force.

Both I_{Kr} (Yang et al., 1997) and heterologously expressed HERG current (Smith et al., 1996) demonstrate inward rectification due to rapid, voltage-dependent inactivation. HERG inactivation resembles the C-type inactivation of Shaker-family K^+ channels (Hoshi et al., 1991) in its sensitivity to extracellular TEA and to mutations in the P-loop (Schonherr and Heinemann, 1996; Smith et al., 1996; Herzberg et al., 1998; Fan et al., 1999). In Shaker, K^+_o and other small extracellular cations slow onset of C-type inactivation (Lopez-Barneo et al., 1993). Raising $[K^+]_o$ may also

---

produce an anti-Nernstian effect on Shaker current magnitude (Lopez-Barneo et al., 1993), but only if the frequency of activating pulses is fast enough that recovery from inactivation between pulses is incomplete (Gomez-Lagunas and Armstrong, 1994; Gomez-Lagunas, 1997). This effect is of K^+_o is quantitatively well-explained by destabilization of the Shaker C-type–inactivated state (Baukrowitz and Yellen, 1995). Raising $[K^+]_o$ was found to slow HERG inactivation (Wang et al., 1996), and it was initially anticipated that the effect of $[K^+]_o$ on HERG current magnitude would be explained entirely by a destabilization of the HERG inactivated state. However, a careful quantitative analysis suggested that the change in inactivation could account for only a small fraction of the observed change in current magnitude. A K^+_o-mediated increase in single-channel conductance was proposed (Wang et al., 1997), consistent with the requirement of very high $[K^+]_o$ for resolution of HERG single-channel events and dependence of single-channel conductance on $[K^+]_o$ over the examined (nonphysiological) range (Kiehn et al., 1996, 1999; Zou et al., 1997, 1998).

Recent studies support an alternative model for the mechanism of $[K^+]_o$ modulation of HERG current, that K^+_o relieves inhibition of HERG current by Na^+_o. This kind of model was first suggested by Scamps and Carmeliet (1989) based on work in rabbit single Purkinje cells before the separation of the delayed rectifier cardiac I_K into I_{Kr} and I_{Ks}, the rapidly activating and slowly activating components (Balser et al., 1990; Sanguinetti and Jurkiewicz, 1990). Working with whole-cell current in a heterologous expression system, we found that extracellular Na^+ (Na^+_o) potently inhibited outward HERG current ($IC_{50} = 3$ mM) in the absence of K^+_o, and the magnitude of current augmentation by K^+_o was markedly reduced in the absence of Na^+_o. Mole fraction experiments revealed a nonadditive interaction between Na^+_o and K^+_o. Although the data did not rule out contributions from direct K^+_o effects on HERG inactivation and single-channel conductance, the magnitude of this effect in the physiologic range of $[K^+]_o$ suggested that the primary mechanism of K^+_o augmentation of HERG current was to relieve inhibition by Na^+_o (Numaguchi et al., 2000a).

The interaction between Na^+_o, K^+_o, and the HERG channel is complex and poorly understood. Recent results from a study focused on antiarrhythmic drug action indicated that $[Na^+]_o$ affects HERG inactivation gating (Numaguchi et al., 2000b). Here we have focused directly on the interaction between Na^+_o and HERG, with a view to developing a more precise biophysical understanding of the Na^+_o effect and thereby illuminating the Na^+_o–K^+_o interaction.

MATERIALS AND METHODS

Plasmid cDNA Constructs

Wild-type HERG cDNA was provided by Dr. Mark Keating (University of Utah, Salt Lake City, UT). DNA for the HERG point mutant S631A was provided by Dr. Michael Sanguinetti (University of Utah). Wild-type and mutant constructs were subcloned into the vector pGFP-IRS for bicistronic expression of the channel protein and GFP reporter as described previously (Johns et al., 1997). The S624A and S624T mutations were generated by PCR using the overlap-extension technique (Tao and Lee, 1994) and subcloned back into our construct.

Cells

Chinese hamster ovary (CHO-K1) cells from the American Type Culture Collection were grown in HAMS F-12 media with L-glutamine (GIBCO BRL), supplemented with 10% fetal bovine serum (GIBCO BRL) and 1% penicillin-streptomycin (GIBCO BRL) in a humidified, 5% CO_2 incubator at 37°C.

Transfection

CHO-K1 cells were transfected using the Lipofectamine (GIBCO BRL) or Fugene 6 (Roche) transfection reagents and method. Cells demonstrating green fluorescence were chosen for electrophysiological analysis.

Solutions

The standard intracellular (pipette) recording solution contained (mM): 110 KCl, 5 K_2ATP, 5 K_4BAPTA, 1 $MgCl_2$, 10 HEPES, adjusted to pH 7.2 with KOH to yield a final intracellular $[K^+]$ of 145 mM.

The extracellular (bath) recording solution contained (mM): 146 XCl (X = sum of K^+, Na^+, and N-methyl-D-glucamine$^+$ [NMDG]), 1 $MgCl_2$, 2 $CaCl_2$, 10 HEPES, 10 glucose, adjusted to pH 7.4 with HCl (low Na^+ solutions) or NaOH (very high Na^+ solutions).

For experiments with $[Na^+]_i$, NaCl was added directly to the standard intracellular solution. Similarly, for experiments with low $[Ba^{2+}_o]$, Ba^{2+} was added directly to extracellular solutions from a 1 M BaCl stock.

Electrophysiology

HERG currents were recorded using the whole-cell patch clamp technique (Hamill et al., 1981). Cells were patch-clamped at room temperature (20–25°C) between 2 and 3 d posttransfection. Recordings used an Axopatch 200B patch clamp amplifier and a Digidata 1200 converter. Pipettes of resistance 2–8 MΩ were fabricated from borosilicate capillary glass (1.5 mm outer diameter, G150F-4; Warner Instrument Corp.) using a Flaming/Brown puller (P-97; Sutter Instrument Co.). Cell and pipette capacitances were nulled and series resistance was compensated (80%) before recording. Data were acquired using pCLAMP6 programs (Axon Instruments, Inc.). Both pCLAMP and Origin (Microcal) programs were used in analyzing and plotting data. For solution exchanges, our 0.5 ml bath was fully exchanged during a 2-min perfusion period before collecting data. Cells were equilibrated to new conditions by pulsing to 20 mV during this period. For most experiments, cells were kept at the holding potential for 6 s between pulses during both the equilibration period and data collection. For the experiments shown in Fig. 9 there was a single extended (90-s) period at the holding potential while solution was exchanged. For the experiments shown in Fig. 12, the time at the holding potential was the independent variable (2, 4, 8, or 16 s). In some experiments, up to three traces from a single cell were

used to generate an average trace used for display (figures) and data analysis. In figures, error bars represent SEM, calculated from several cells. P values in the text and figure legends are from independent Student's t tests. In some cases, one-population t tests were used to compare a normalized statistic to a mean of 0 or 1. No current rundown was observed for as long as 1 h. Na^+_o effects could be washed out completely with our solution exchange setup.

Generating Structural Hypotheses Based on the KcsA Crystal Structure

Fig. 13, which illustrates a putative structural effect of the S624A mutation, was created using the KcsA crystal structure coordinates, accession code 1BL8 (Doyle et al., 1998) and Insight II modeling software (Molecular Simulations, Inc.) on a Silicon Graphics O_2 workstation. Putative hydrogen bonds were identified using a heavy-atom distance criterion of <3 Å.

R E S U L T S

Voltage Dependence of Current Inhibition by Extracellular Sodium: Absence of a Predominant Field Effect

To characterize the voltage dependence of HERG current inhibition by Na^+_o, we measured the inhibitory potency of Na^+_o in the absence of K^+_o at several membrane potentials (Fig. 1). 2-s depolarizing steps to a variable test potential were followed by a 2-s step to −50 mV. Channels open and inactivate in response to the depolarizing test step. The step to −50 mV elicits hooked "tail currents" due to fast recovery from inactivation, followed by slower deactivation. We chose to use 3 mM Na^+_o because it is near the IC_{50} for current inhibi-

tion at 20 mV (Numaguchi et al., 2000a). Therefore, any effects of membrane potential on inhibition are expected to be most prominent at this concentration, as 3 mM corresponds to the steepest part of the dose-response curve. Fig. 1, A and B, show results from an experiment in a single cell recorded in 0 Na^+_o and 3 mM Na^+_o, respectively. Data summarizing current levels at the end of the 2-s depolarizing test step (Fig. 1, A and B, arrows) are summarized in Fig. 1 C. Current at each test potential was normalized to the value in 0 Na^+_o in the same cell. We observed a modest trend toward increasing Na^+_o inhibition with greater depolarization (44 ± 3% inhibition of current at 0 mV vs. 55 ± 3% at 40 mV, $n = 7$, P < 0.05). Notably, this trend was opposite in direction to the expectation for a simple field effect, which would predict greater inhibition at more hyperpolarized potentials. A balance between an inhibition-promoting effect of a depolarization-induced conformational change and an inhibition-opposing field effect could potentially explain the plateau in the voltage-inhibition curve (Fig. 1 C, 40–80 mV). Alternatively, the Na^+_o binding site could be located outside the transmembrane field with a small effect of channel conformational state accounting for the observed trend.

HERG P-loop Mutants with Impaired Inactivation Are Relatively Insensitive to Inhibition by Extracellular Sodium

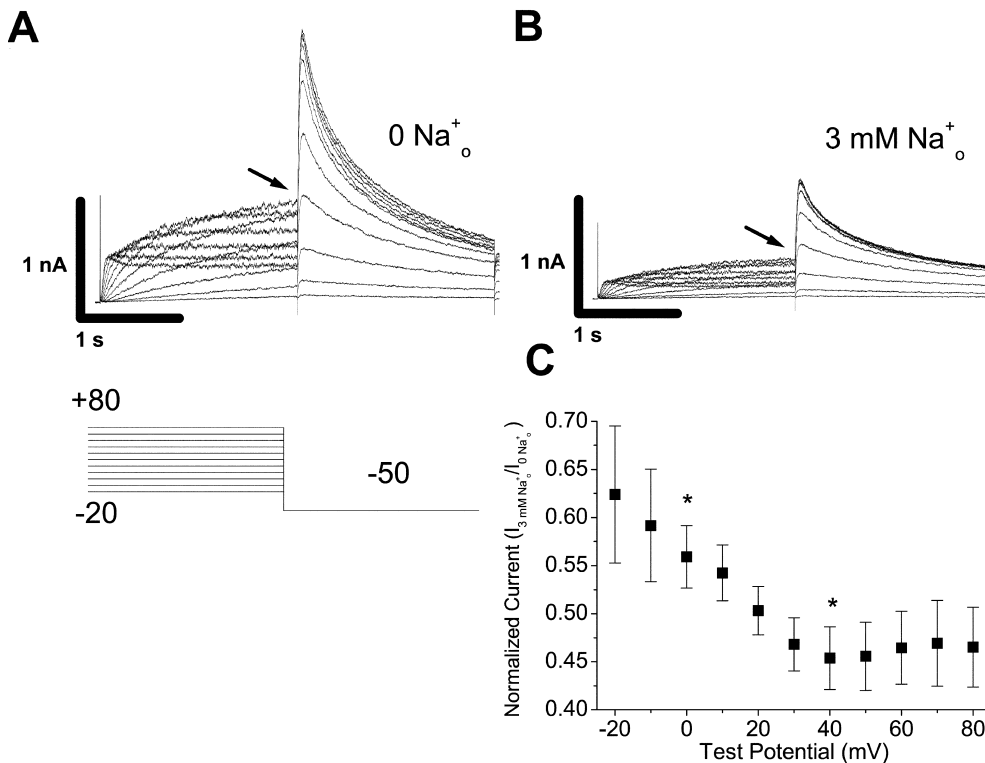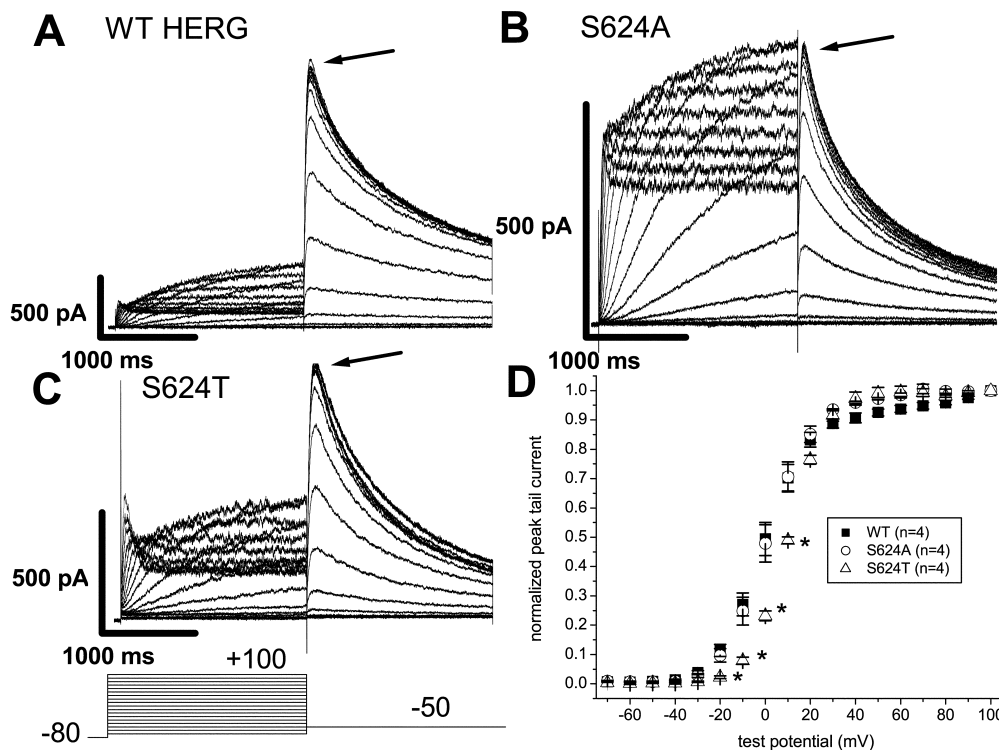To gain insight into the structural basis and possible conformational-state dependence of HERG's Na^+_o sen-

FIGURE 1. Effect of test potential on current inhibition by Na^+_o. Membrane potential was stepped from −80 mV to a test potential between −20 and 80 mV for 2 s, followed by stepoff to −50 mV. (A and B) Representative traces from a paired experiment in which a single cell was moved from 0 Na^+_o to 3 mM Na^+_o with $[K^+]_o$ held at 0. (C) Relationship of test potential to current inhibition by 3 mM Na^+_o. Current in 3 mM Na^+_o at the end of the 2-s depolarizing test step (B, arrow) was normalized to the value in 0 Na^+_o (arrow, A) at each test potential for several cells ($n = 7$). Normalized current differed significantly at only one pair of tested voltages, 0 mV vs. 40 mV (P < 0.05). Note that the observed trend of increasing inhibition at more depolarized test potentials is opposite the expectation for a simple field effect.

FIGURE 2. Baseline isochronal activation of WT, S624A, and S624T HERG channels. Membrane potential was stepped from −80 mV to a test potential between −70 and 100 mV for 2 s, followed by stepoff to −50 mV, to assess the voltage dependence of channel activation in 0 Na^+_o, 0 K^+_o. A–C show representative families of current for WT HERG (closed squares), S624A (open circles), and S624T (open triangles), respectively. Peak tail current at −50 mV provides a measurement of the number of activated channels at each test potential. Peaks were normalized to the peak following the pulse to 100 mV, and data from several cells are summarized in D. The voltage dependence of activation for WT HERG and S624A was indistinguishable in the steep voltage-dependent region, whereas the voltage dependence of activation for S624T was significantly shifted in the positive direction for potentials between −20 mV and 10 mV (P < 0.05 vs. WT).

sitivity, we studied the Na^+_o sensitivity of several HERG mutants. We chose to focus our attention initially on mutations in the pore-lining, P-loop region. Several HERG P-loop mutations completely derange both K^+ selectivity and inactivation gating (Smith et al., 1996; Herzberg et al., 1998; Fan et al., 1999). Although such effects could be consistent with a mechanism in which Na^+_o preferentially interacts with the HERG inactivated state, the permeability of these mutant channels to Na^+ limits their utility for studying inhibition of outward HERG K^+ current by Na^+_o. Therefore, we chose to focus on mutant channels that retained K^+ selectivity in standard solution conditions. The point mutants we studied included S631A, a channel with a well-characterized gating phenotype (Schonherr and Heinemann, 1996; Zou et al., 1998), as well as S624A and S624T, which are not well-characterized. S631A HERG channels retain K^+ selectivity and have voltage dependence of activation identical to that of WT HERG, but inactivation in S631A is shifted by 100 mV relative to WT (Zou et al., 1998). The S624A mutation was one of several reported to influence methanesulfonanilide block in an alanine-scanning mutagenesis study (Mitcheson et al., 2000a), but its gating has not been studied in detail. To our knowledge, no phenotype of S624T has been described previously.

Fig. 2 compares the responses of WT, S624A, and S624T mutant channels to a standard HERG activation protocol similar to the one shown in Fig. 1. The extra-cellular solution was 0 Na^+_o, 0 K^+_o, so the experiment provides a measure of "baseline" channel kinetics independent of external cation concentrations. The morphology of S624A and S624T HERG currents (Fig. 2, B and C, respectively) immediately suggests impaired inactivation compared with WT (Fig. 2 A). Specifically, in the mutants, current at depolarized test potentials is more similar in magnitude to peak tail current than in WT HERG, for which peak tail currents are much larger. The protocol in Fig. 2 does not provide a distinct measurement of inactivation gating, but does allow for comparison of the voltage dependence of activation in mutant and WT channels. Because recovery from inactivation is faster than channel deactivation, peak tail current (Fig. 2, A–C, arrows) provides a measure of the number of activated channels at each test potential. These values were normalized to the peak tail after a test pulse of 100 mV, and results from several experiments are summarized in Fig. 2 D. The voltage dependence of activation for WT and S624A channels was quite similar, whereas activation of S624T was significantly shifted in the depolarizing direction for potentials between −20 and 10 mV.

The experiments in Fig. 3 more directly addressed the voltage dependence of inactivation in S624A and S624T. We applied a triple-pulse protocol (Smith et al., 1996; Spector et al., 1996) in the absence of Na^+_o and K^+_o to compare the "baseline" partitioning of channels between open and inactivated states in WT and mutant
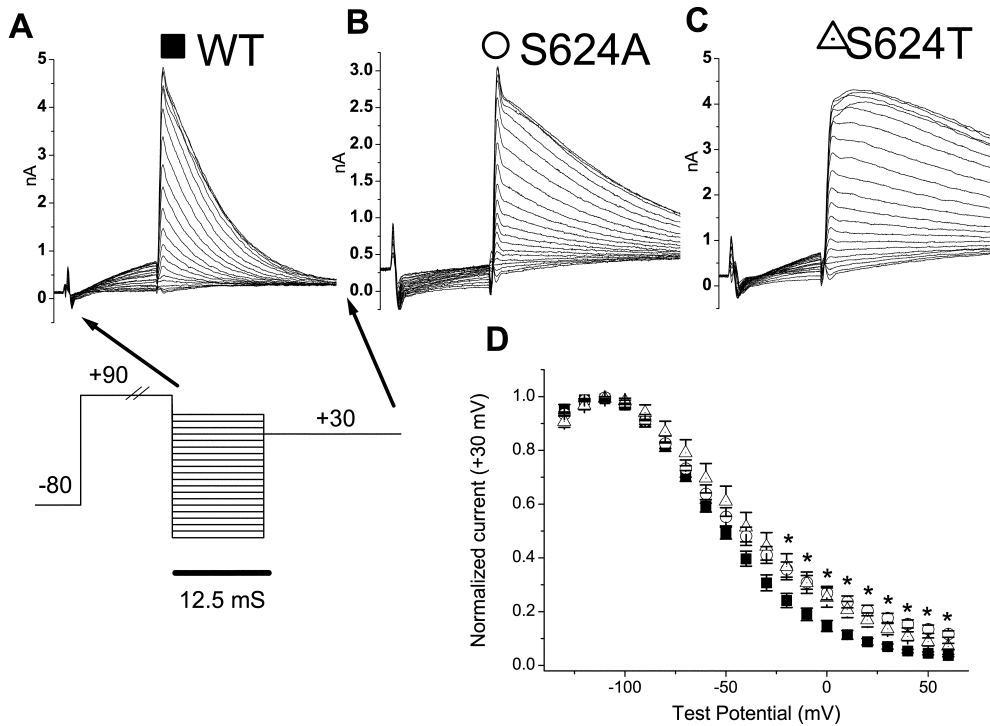
FIGURE 3. Baseline steady-state inactivation of WT, S624A, and S624T HERG channels. A "triple-pulse" voltage clamp protocol (Smith et al., 1996; Spector et al., 1996) was used to assess the voltage dependence of channel availability in 0 Na^+_o, 0 K^+_o. A–C show typical families of currents at the test potential and a subsequent step to 30 mV for WT HERG (closed squares), S624A (open circles), and S624T (dotted triangles), respectively. Peak current observed immediately after stepping to 30 mV was normalized to the largest peak current recorded in the same cell. Data from several cells ($n = 4$ for each channel) are summarized in D. At test potentials greater than -20 mV for S624A and greater than -10 mV for S624T, normalized current was significantly greater than that observed for WT HERG ($P < 0.05$), consistent with impaired inactivation relative to WT.

channels. A strong, extended initial depolarizing step inactivated most channels. Channels then equilibrated between open and inactivated states during a short (12.5-ms) step to the test potential. Finally, the number of open channels was measured immediately after stepping to 30 mV (Fig. 3, A–C, symbols). By this measurement, both S624A and S624T channels have significantly decreased baseline inactivation compared with WT channels over a range of depolarized voltages (Fig. 3 D). Slower onset of inactivation for S624A and S624T was also visible in the representative traces shown (Fig. 3, A–C, compare current decay after final step to 30 mV).

The gating phenotypes of S624A and S624T can be summarized as follows. For both mutants, inactivation was significantly impaired (vs. WT) at potentials greater than or equal to -20 mV (Fig. 3). For S624A, voltage dependence of activation was similar to WT HERG. For S624T, there were significantly fewer activated channels at potentials between -20 and 10 mV (Fig. 2).
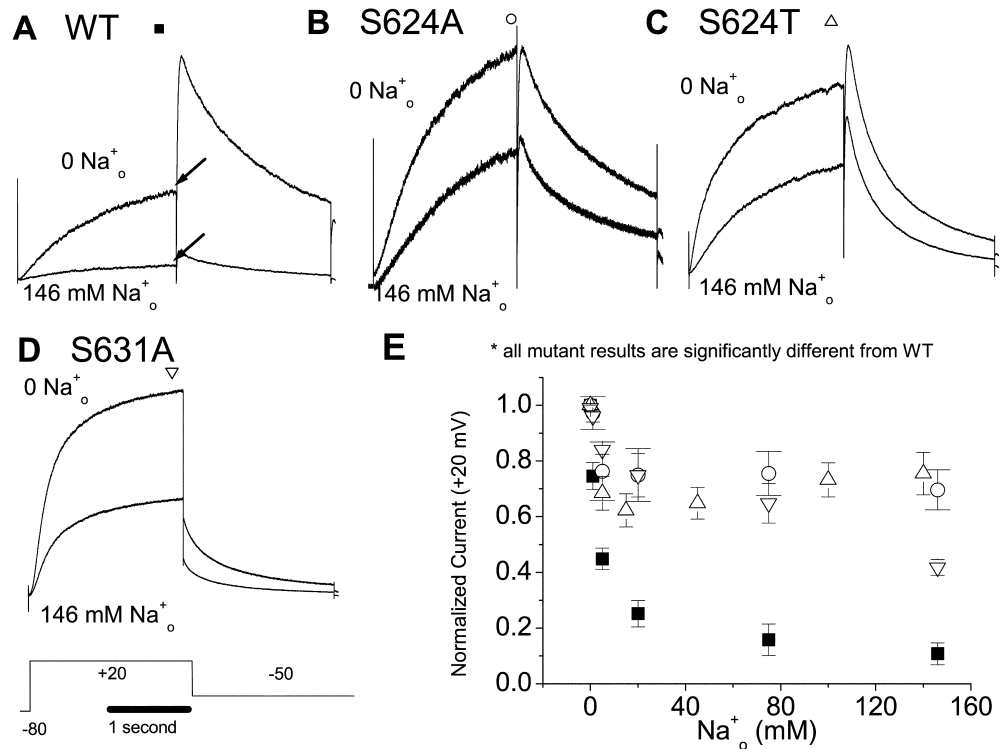
Overall, for potentials of 20 mV and higher, S624A and S624T have significantly impaired inactivation compared with WT, but are not significantly different from WT with respect to activation.

Having characterized the gating phenotype of S624A and S624T, we next studied the sensitivity of these channels and S631A channels to inhibition by Na^+_o

(Fig. 4). We compared currents at 20 mV in several $[Na^+]_o$, all in the absence of K^+_o. Representative traces for WT HERG, S624A, S624T, and S631A are shown in Fig. 4, A–D, respectively. Note the large outward tail currents in S624A (Fig. 4 B) and S624T (Fig. 4 C) present at -50 mV even in very high (146 mM) $[Na^+]_o$. This feature is indicative not only of reduced sensitivity of these mutant channels to inhibition by Na^+_o, but also of their high K^+ selectivity. For each record in Na^+_o, current at the end of the 2-s step was normalized to the value from the same cell in 0 Na^+_o. Data from several cells are summarized in Fig. 4 E. The three mutant channels each demonstrated significantly reduced sensitivity to inhibition by Na^+_o versus WT at all concentrations studied. Interestingly, the dose-response relationships for the three mutant channels are quite similar, and for S624A and S624T the relationships appear to reach a plateau far short of complete inhibition (Fig. 4 E). This result is not easily explained, but we offer a possible interpretation in the discussion, informed by data presented later in the paper.

The sensitivity of Na^+_o inhibition to P-loop mutations (Fig. 4) would be expected if Na^+_o bound to a site in the HERG pore. However, the lack of a predominant field effect on Na^+_o inhibition (Fig. 1) and the correlation of potent Na^+_o inhibition with an intact inactivation mechanism (Fig. 4) are also potentially consistent

FIGURE 4. Sensitivity of WT and mutant HERG current to inhibition by Na^+_o. Cells were held at -80 mV and subsequently stepped to 0 mV for 2 s, followed by a 2-s step to -50 mV. In each experiment, currents were recorded first in 0 K^+_o, 0 Na^+_o and all data from a given cell were normalized to this measurement. Individual cells were washed through several solutions with varying $[Na^+]_o$ while $[K^+]_o$ was held at 0. Current (y-axis) scales are not shown; none of the traces exceeded 2 nA. Three mutant channels with impaired inactivation were tested. Representative currents from WT HERG (filled squares), S624A (open circles), S624T (upward triangles), and S631A (downward triangles) are shown in A–D, respectively. Normalized data from several cells (current at the end of the 2-s depolarizing step (top, see arrows in A) are summarized in E, which compares the Na^+_o dose-response relationships for the four channels tested. The mutant channels with impaired inactivation were significantly less sensitive to inhibition by Na^+_o throughout the tested range of $[Na^+]_o$ ($n = 3$–7 for each point, $P < 0.05$ for each mutant channel compared with WT at each concentration).

with Na^+_o acting allosterically to stabilize the inactivated state at a site remote from the pore. Further, it is also conceivable that Na^+_o could stabilize the inactivated state by binding in the pore. We chose to utilize intracellular Na^+ (Na^+_i) and extracellular barium (Ba^{2+}_o) as probes to begin to define the location of a binding site for Na^+_o. We considered three possibilities for the site of Na^+_o action: inner pore, outer pore, and remote from the pore.

Intracellular Sodium Inhibits HERG Current in a Manner Consistent with Voltage-dependent Block and Independent of Extracellular Sodium

The action of intracellular Na^+ (Na^+_i) to block voltage-gated K^+ currents is well described (Bezanilla and Armstrong, 1972; French and Wells, 1977; Yellen, 1984a,b) and, in light of the KcsA crystal structure (Doyle et al., 1998), interpreted to occur in a large intracellular cavity (Heginbotham et al., 1999; Zhou et al., 2001). A macroscopic Na^+_i block with features in common with previous descriptions of Na^+_i block (Bezanilla and Armstrong, 1972; French and Wells, 1977; Yellen, 1984a,b), including antagonism by K^+_o, was reported recently for the I_{Ks} (KCNQ1/KCNE1) channel (Pusch et al., 2001).

We have suggested several nonexclusive possibilities for the mechanism of Na^+_o inhibition of outward HERG K^+ current. As a prerequisite to limiting the number of possible models, we considered approaches that could potentially identify the region of the channel where Na^+_o acts. Reasoning that observation of similar effects of Na^+_i and Na^+_o on the HERG channel would implicate the pore, we examined the impact of Na^+_i on HERG channel function.

Fig. 5, A and B, show the basic effect of adding 10 mM Na^+ to the standard (high-K^+) pipette solution on WT HERG currents. Results from several cells, quantified as the ratio of current measured at a depolarized potential to the peak tail current, are summarized in Fig. 5 C. Addition of 10 mM Na^+ to the pipette solution significantly reduced this ratio compared with the standard internal solution (at 20 mV, 0.39 ± 0.04 vs. 0.14 ± 0.01 for 0 and 10 mM Na^+_i, respectively, $P < 0.01$), consistent with current inhibition at depolarized potentials and/or an increase in current at hyperpolarized potentials. Current magnitude at depolarized potentials was significantly smaller in the presence of 10 mM Na^+_i. The change in magnitude of current at depolarized potentials when 10 mM Na^+_i was included (Fig. 5 D) closely resembled the change in current ratio with Na^+_i (Fig. 5 C). This suggested that the change in ratio primarily reflected current inhibition by Na^+_i at depolarized potentials. We next tested the effect of Na^+_i on the magnitude of current augmentation by K^+_o (Fig. 6).
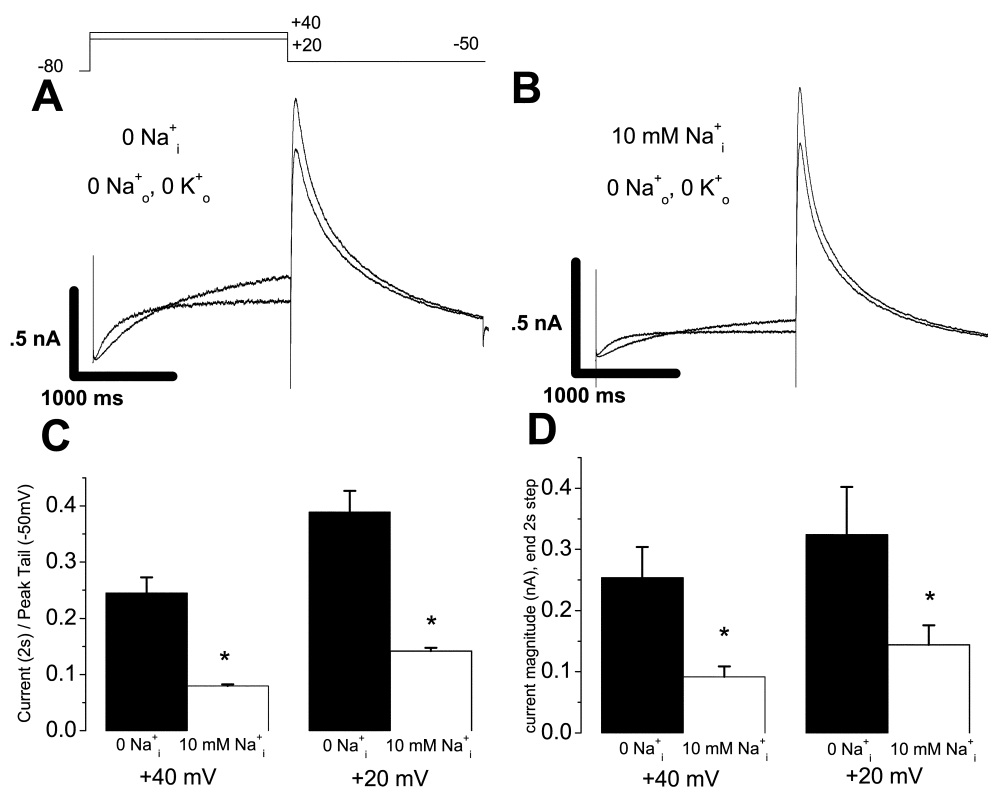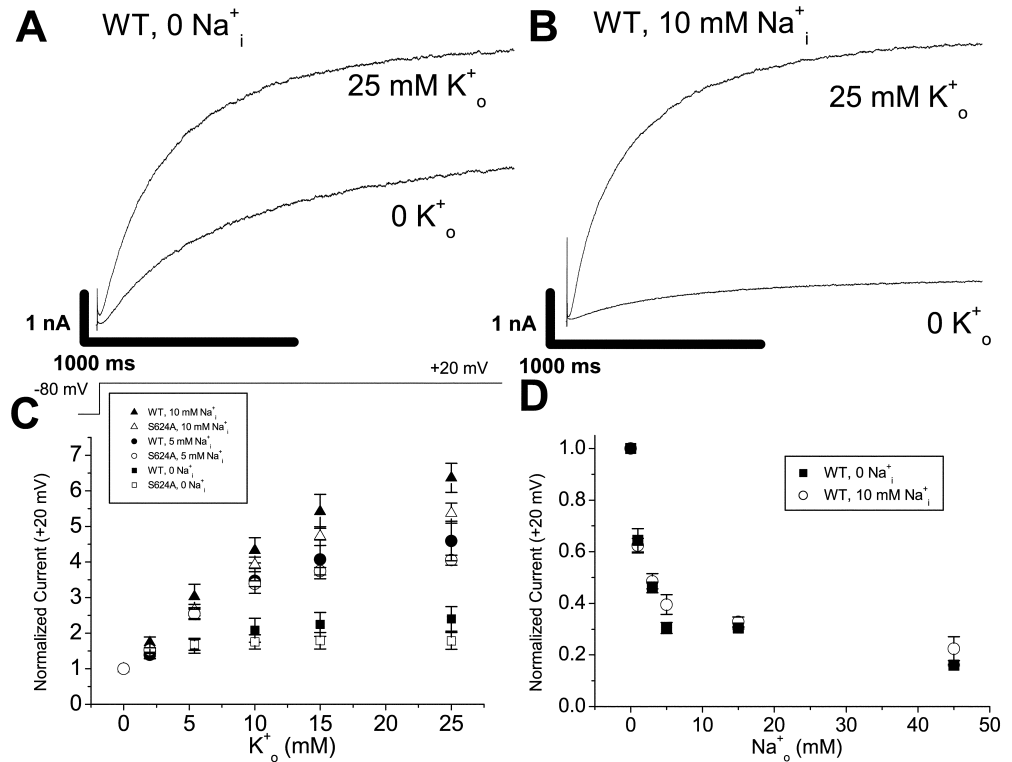
FIGURE 5. Effect of 10 mM Na^+_i on WT HERG currents. Cells were stepped from a holding potential of -80 mV to a test potential of 20 or 40 mV for 2 s, followed by a 2-s step to -50 mV. (A and B) Representative (unpaired) cells recorded in the absence (A) and presence (B) of 10 mM Na^+_i. (C) Data from several experiments as in A ($n = 5$) and B ($n = 9$) are summarized as the ratio of current at the end of the 2-s test step to the peak tail current at -50 mV. This ratio was significantly smaller in the presence of 10 mM Na^+_i at both test potentials (P $<$ 0.01). (D) Effect of Na^+_i on current magnitude at the end of the 2-s depolarizing step. Current magnitude was significantly smaller in the presence of 10 mM Na^+_i at both test potentials (P $<$ 0.03), and observations were collected from the same cells used to generate the data in Fig. 5 C.

Given the ability of K^+_o to relieve current inhibition by Na^+_o (Numaguchi et al., 2000a), a simple model in which Na^+_i acts by the same mechanism as Na^+_o predicts that the magnitude of current augmentation by K^+_o will be greater in the presence of Na^+_i. Notably, K^+_o has also been reported to relieve Na^+_i inhibition in other voltage-gated K^+ channels (Bezanilla and Armstrong, 1972; Yellen, 1984a,b; Pusch et al., 2001). Fig. 6, A and B, show results from representative cells expressing WT HERG in 0 Na^+_i and 10 mM Na^+_i, respectively. Maximum current augmentation by K^+_o was more than sixfold in the presence of 10 mM Na^+_i and approximately twofold with the standard (0 Na^+) internal solution (Fig. 6 C). The significant reduction in current magnitude in cells with 10 mM Na^+_i in the absence of K^+_o (see Fig. 5 D, also compare traces in Fig. 6, A and B) suggests that the data should be interpreted as relief of Na^+_i block by K^+_o rather than enhancement of a K^+_o effect by Na^+_i. Further, the change shown in Fig. 5 D is a 2–3-fold reduction in current magnitude in the presence of 10 mM Na^+_i, which corresponds to the threefold increase in the magnitude of the K^+_o augmentation effect when 10 mM Na^+_i is present (Fig. 6 C). The observation that physiologically relevant $[Na^+]_i$ inhibited HERG current in a manner sensitive to physiologically relevant $[K^+]_o$ (note low $[K^+]_o$ region of graph, Fig. 6 C) is interesting and will be revisited in the discussion.

Using current augmentation by K^+_o as an index of sensitivity to inhibition by Na^+_i, we also tested the effect of Na^+_i on the S624A channel (Fig. 6 C). A simple model in which Na^+_i and Na^+_o both act at an inner pore site that predicts that S624A channels, shown to have decreased sensitivity to inhibition by Na^+_o (Fig. 4, B and E), will also have reduced sensitivity to inhibition by Na^+_i. Instead, S624A and WT channels had very similar sensitivity to Na^+_i, as inferred from K^+_o augmentation (Fig. 6 C). Further, the small difference may be attributable to an intrinsic difference in K^+_o sensitivity independent of Na^+_i (see 25 mM K^+_o in the absence of Na^+_o, Fig. 6 C). This result suggests that Na^+_o and Na^+_i act by fundamentally different mechanisms. We also measured the effect of Na^+_i on the potency of current inhibition by Na^+_o. Na^+_o inhibition appeared unaffected by 10 mM Na^+_i (Fig. 6 D). This result is also consistent with different mechanisms for Na^+_o and Na^+_i. It is theoretically possible that Na^+_o and Na^+_i could act at the same (internal) site with inactivation serving as a rate-limiting determinant of Na^+_o access to the site. However, given the similar Na^+_i effect in S624A and WT HERG (Fig. 6 C), this interpretation requires that the S624A mutation impair inactivation without changing the structure of the relevant pore site. Further, this interpretation also requires that a 10–15% difference in steady-state inactivation (see Fig. 3 D) be translatable to a difference of up to 50% in fractional site occupancy (see Fig. 4 E).

Overall, the features of the Na^+_i inhibition of HERG, including sensitivity to K^+_o, are broadly consistent with the kind of voltage-dependent block by Na^+_i described for other K^+ channels (Bezanilla and Armstrong, 1972; French and Wells, 1977; Yellen, 1984a,b; Pusch et al., 2001) and interpreted to occur in the cavity (Heginbotham et al., 1999; Zhou et al., 2001). Moreover, Na^+_i and Na^+_o appear to act by distinct mechanisms. Thus, Na^+_o is unlikely to act by reaching the inner pore or cavity of HERG. These experiments using Na^+_i as a probe do not shed light on the question of whether Na^+_o reaches the outer pore or acts at a remote site. Therefore, we employed an alternative probe, Ba^{2+}, to further investigate the location of the Na^+_o receptor.

Barium Attenuates Current Inhibition by Extracellular Sodium, and Extracellular Sodium Slows Barium Egress from the Channel

Barium (Ba^{2+}) was used as a probe in a pair of elegant studies (Neyton and Miller, 1988a,b) that predicted the K^+ channel pore structure (Doyle et al., 1998; Jiang and MacKinnon, 2000; Morais-Cabral et al., 2001; Zhou et al., 2001) based on functional data. Extracellular barium (Ba^{2+}_o) block of HERG exhibits strong voltage dependence consistent with a binding site deep in the pore (Ho et al., 1999; Weerapura et al., 2000), similar

to the site now confirmed crystallographically for KcsA (Jiang and MacKinnon, 2000). Classical C-type inactivation traps Ba^{2+} in the channel (Basso et al., 1998; Harris et al., 1998), whereas HERG channel inactivation relieves Ba^{2+}_o block with kinetics that are measurable (Weerapura et al., 2000). Here, we utilize this unusual interaction between Ba^{2+} and HERG inactivation to distinguish between a model in which Na^+_o reaches the HERG pore and a simple remote allosteric model in which Na^+_o stabilizes the inactivated state. Our experimental design was a macroscopic version of an approach first employed by Neyton and Miller (1988b) in single channel measurements of BK channels. This approach is to measure the effects of external cations on the rate of Ba^{2+} egress at depolarized potentials. For a classical C-type–inactivating channel, the interpretation of a result in which Na^+_o slows Ba^{2+} egress would be problematic because of the potential trapping of Ba^{2+} by C-type inactivation. For HERG, however, a result in which Na^+_o slows Ba^{2+} egress would be informative, and would strongly support a pore-occluding model for current inhibition. The prediction of the remote allosteric model is that Na^+_o will speed relief of Ba^{2+}_o block by promoting HERG channel inactivation. Notably, a speeding of Ba^{2+} egress could also be consistent with a pore-occluding model. For example, Na^+_o binding in
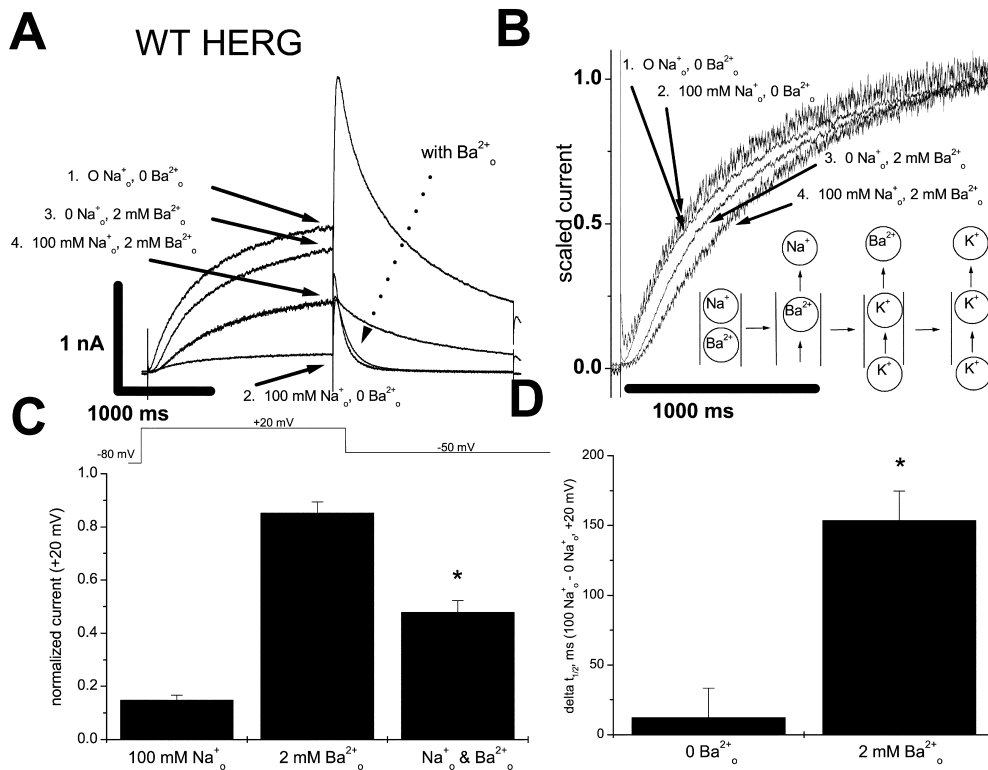
FIGURE 7. Effects of combining $Ba^{2+}{}_o$ and $Na^+{}_o$ in WT HERG. Cells were stepped from a holding potential of -80 to 20 mV for 2 s, followed by a 2-s step to -50 mV. $[K^+]_o$ was held at 0 in these experiments. (A) Representative WT currents from a cell washed through four consecutive solutions as shown. Dotted arrow indicates fast tail current decay in presence of $Ba^{2+}{}_o$, reflecting $Ba^{2+}{}_o$ loading at hyperpolarized potentials. (B) currents from A at 20 mV scaled to show the rate of current rise. Arrows indicate the $t_{1/2}$ (time to half-maximal current value). The cartoon underneath the scaled traces illustrates the simplest model that can explain the data. In this model, $Na^+{}_o$ inhibits Ba^{2+} egress by occupying a site external to the Ba^{2+} site (explaining the effect on normalized $t_{1/2}$) and Ba^{2+} clears $Na^+{}_o$ as it exits the pore (explaining the relief of $Na^+{}_o$ inhibition by $Ba^{2+}{}_o$). With both Ba^{2+} and Na^+ cleared from the pore, K^+ ions can move through the channel. Note that inactivation is not shown explicitly here. (C) For several cells as in A ($n = 7$), current at the end of the 2-s depolarizing step (A, solid arrows) was normalized to the value in 0 $Na^+{}_o$, 0 $Ba^{2+}{}_o$. Normalized current in 100 mM $Na^+{}_o$ alone and 2 mM $Ba^{2+}{}_o$ alone was smaller than one ($P < 0.02$ in both cases), yet current in 100 mM $Na^+{}_o$ + 2 mM $Ba^{2+}{}_o$ was significantly greater than current in 100 mM $Na^+{}_o$ alone ($P < 0.01$). (D) For several cells as in B ($n = 7$), $\Delta t_{1/2}$ values were calculated by subtracting the $t_{1/2}$ in 0 $Na^+{}_o$ from the $t_{1/2}$ in 100 mM $Na^+{}_o$. The calculation was made for 0 and 2 mM $Ba^{2+}{}_o$ and results were compared. Although $\Delta t_{1/2}$ in 0 $Ba^{2+}{}_o$ was indistinguishable from 0 ($P = 0.58$), the $\Delta t_{1/2}$ in 2 mM $Ba^{2+}{}_o$ was significantly greater than the value in 0 $Ba^{2+}{}_o$ ($P < 0.001$). An alternative way to analyze the data is to run paired t tests on the raw $t_{1/2}$ values (0 $Na^+{}_o$, 0 $Ba^{2+}{}_o$ vs. 100 mM $Na^+{}_o$, 0 $Ba^{2+}{}_o$ and 0 $Na^+{}_o$, 2 mM $Ba^{2+}{}_o$ vs. 100 mM $Na^+{}_o$, 2 mM $Ba^{2+}{}_o$). This approach yields the same inferences regarding statistical significance as independent t tests on the $\Delta t_{1/2}$ values.

the pore could destabilize Ba^{2+} via a repulsive mechanism. If the off-rate for $Na^+{}_o$ were faster than the Ba^{2+} off-rate, then such a mechanism might explain $Na^+{}_o$ speeding of Ba^{2+} egress even for the case in which Ba^{2+} leaves to the outside (as expected at a depolarized potential favoring K^+ efflux). Another possibility is that $Na^+{}_o$ could stabilize the HERG inactivated state by binding in the pore; in that case, the effect of $Na^+{}_o$ on speed of Ba^{2+} egress would depend on the relative importance of conformational state and pore occlusion.

It follows that the most informative result for the experiment combining $Na^+{}_o$ and $Ba^{2+}{}_o$ would be a slowing of $Ba^{2+}{}_o$ egress by $Na^+{}_o$. In the case that $Na^+{}_o$ slows Ba^{2+} egress, the only alternative to inferring that $Na^+{}_o$ occludes the pore is to speculate that $Na^+{}_o$ remotely stabilizes a heretofore undefined state that locks $Ba^{2+}{}_o$ in the pore. The predictions of pore-occluding and remote allosteric models regarding the effects of combining $Na^+{}_o$ and $Ba^{2+}{}_o$ on current magnitude are also of interest. A pore-occluding model predicts that $Ba^{2+}{}_o$ will relieve $Na^+{}_o$ inhibition of HERG current, in that

Ba^{2+} would sweep Na^+ from the pore as it leaves inactivated channels. The remote allosteric model, by contrast, does not make a straightforward prediction as to the effect of combining $Ba^{2+}{}_o$ and $Na^+{}_o$ on current magnitude.

Some K^+ channels require channel opening to be blocked by $Ba^{2+}{}_o$ (Miller et al., 1987), whereas others are susceptible to $Ba^{2+}{}_o$ block while closed (Armstrong and Taylor, 1980; Armstrong et al., 1982; Hurst et al., 1995; Harris et al., 1998). In either case, Ba^{2+} can remain bound in the pore when the channel closes (Armstrong and Taylor, 1980; Armstrong et al., 1982; Miller, 1987; Miller et al., 1987; Hurst et al., 1995; Harris et al., 1998). Ba^{2+} appears to have similar affinity for the open and closed states of HERG (Weerapura et al., 2000). In our experiments, channels are pulsed continuously and the results shown are at steady-state (see MATERIALS AND METHODS). Therefore, whether or not $Ba^{2+}{}_o$ can enter closed HERG channels, a percentage of open HERG channels are "loaded" with Ba^{2+} at hyperpolarized potentials before each depolarizing pulse.

FIGURE 8. Effects of combining Ba^{2+}_o and Na^+_o in HERG S624A. Cells were stepped from a holding potential of -80 to 20 mV for 2 s, followed by a 2-s step to -50 mV. $[K^+]_o$ was held at 0 in these experiments. (A) Representative S624A currents from a cell washed through four consecutive solutions as shown. (B) Currents from A at 20 mV scaled to show the rate of current rise. Arrows indicate the $t_{1/2}$ (time to half-maximal current value). (C) for several cells as in A ($n = 5$), current at the end of the 2-s depolarizing step (A, arrows) was normalized to the value in 0 Na^+_o, 0 Ba^{2+}_o. Normalized current for S624A in 2 mM Ba^{2+}_o was significantly smaller than the value for WT in 2 mM Ba^{2+}_o (compare with Fig. 7 C, P < 0.01). Normalized S624A current in 100 mM Na^+_o + 2 mM Ba^{2+}_o was significantly smaller

than the S624A values in 100 mM Na^+_o alone (P = 0.05) and 2 mM Ba^{2+}_o alone (P < 0.01). (D) For several cells as in B ($n = 5$), Δ $t_{1/2}$ values were calculated by subtracting the $t_{1/2}$ in 0 Na^+_o from the $t_{1/2}$ in 100 mM Na^+_o. The calculation was made for 0 and 2 mM Ba^{2+}_o, and results were compared. Δ $t_{1/2}$ was greater than 0 for both 0 Ba^{2+}_o and 2 mM Ba^{2+}_o (P < 0.01 in both cases), but the values in 2 mM Ba^{2+}_o and 0 Ba^{2+}_o were indistinguishable from one another (P = 0.55).
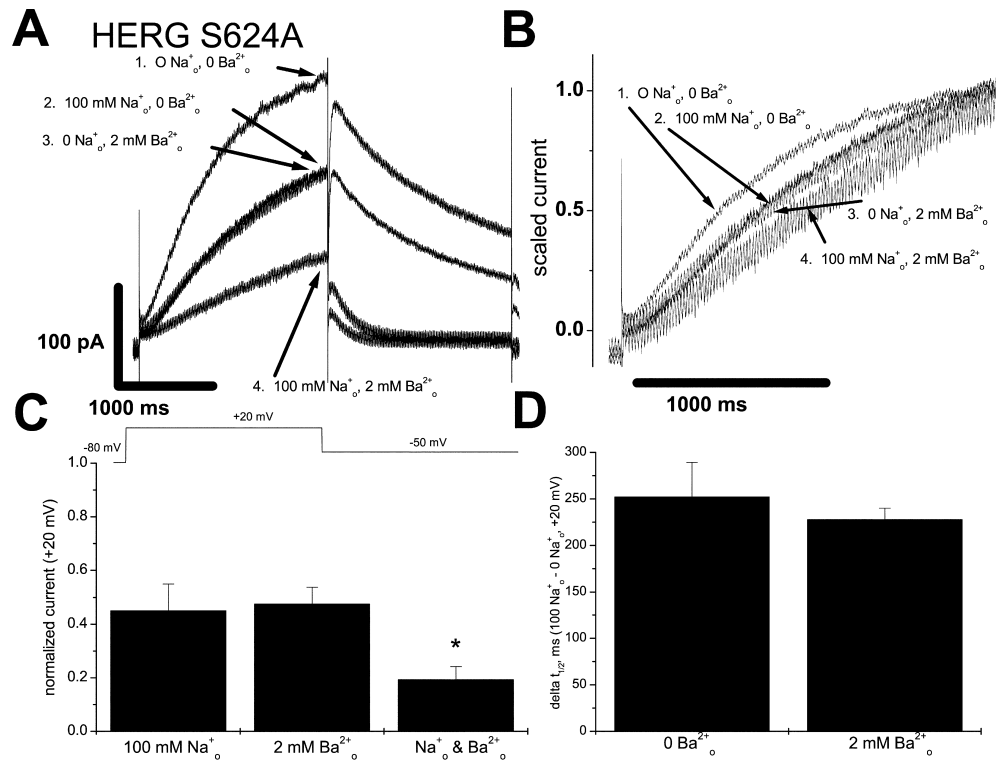
The fast tail current decay in the presence of Ba^{2+} (dotted arrow, Fig. 7 A) reflects this loading.

In the first experiment with Ba^{2+}_o, individual cells were recorded in four different external solution conditions (all 0 K^+_o): (a) 0 Na^+_o, 0 Ba^{2+}_o, (b) 100 mM Na^+_o, 0 Ba^{2+}_o, (c) 0 Na^+_o, 2 mM Ba^{2+}_o, (d) 100 mM Na^+_o, 2 mM Ba^{2+}_o. Two major effects of combining Na^+_o and Ba^{2+}_o were observed: (a) Ba^{2+}_o attenuates Na^+_o inhibition (Fig. 7, A and C), and (b) Na^+_o slows Ba^{2+}_o egress as reflected in a delay in the current rise time (Fig. 7, B and D). Fig. 7, A and B, show raw current records from a representative cell. Records are scaled in Fig. 7 B to accentuate the similarities and differences in rate of current rise.

Although 2 mM Ba^{2+} alone caused a small reduction in the current at the end of a 2s pulse compared with baseline (0 Na^+_o, 0 Ba^{2+}_o), current in 2 mM Ba^{2+}_o + 100 mM Na^+_o was significantly greater than current in 100 mM Na^+_o alone (Fig. 7 C). This effect of Ba^{2+}_o to relieve Na^+_o inhibition was dramatic, yielding approximately threefold more current than was seen for Na^+_o alone (mean I_{norm}= 0.48 ±.04 vs. 0.15 ± 0.02 for 100 mM Na^+_o alone).

Because many current records did not reach steady-state by the end of a 2-s pulse, we quantified the rate of current rise (which we interpret to reflect the rate of

Ba^{2+} egress) using a $t_{1/2}$ measurement (the time necessary for current to reach half of its end level, see Fig. 7 B, arrows). 100 mM Na^+ alone did not affect the $t_{1/2}$ measurement (compared with 0 Na^+_o, 0 Ba^{2+}_o), but 100 mM Na^+_o + 2 mM Ba^{2+}_o did significantly increase the $t_{1/2}$ compared with 2 mM Ba^{2+} alone (Fig. 7 D). The results of these experiments, then, indicated that Na^+_o and Ba^{2+}_o effects are not functionally independent. The data suggested a model in which Na^+_o inhibits Ba^{2+} egress by occupying a site external to the Ba^{2+} site (explaining the effect on $t_{1/2}$) and Ba^{2+} clears Na^+_o as it exits the pore (explaining the relief of Na^+_o inhibition by Ba^{2+}_o). This model is illustrated in the cartoon shown under the scaled currents in Fig. 7 B.

Barium Relief of Current Inhibition by Extracellular Sodium Is Absent in the Inactivation-impaired Mutant S624A

We performed Ba^{2+}_o-Na^+_o combination experiments similar to those described for WT in the point mutant S624A, which is impaired in both inactivation (Fig. 3 D) and Na^+_o sensitivity (Fig. 4 E). Fig. 8, A and B, show raw and scaled current traces, respectively, and Fig. 8, C and D, summarize current magnitude and $t_{1/2}$ data, respectively. The model of Ba^{2+}_o action proposed by Weerapura et al. (2000), who studied effects of Ba^{2+}_o on the inactivation-impaired mutant S631A, predicts
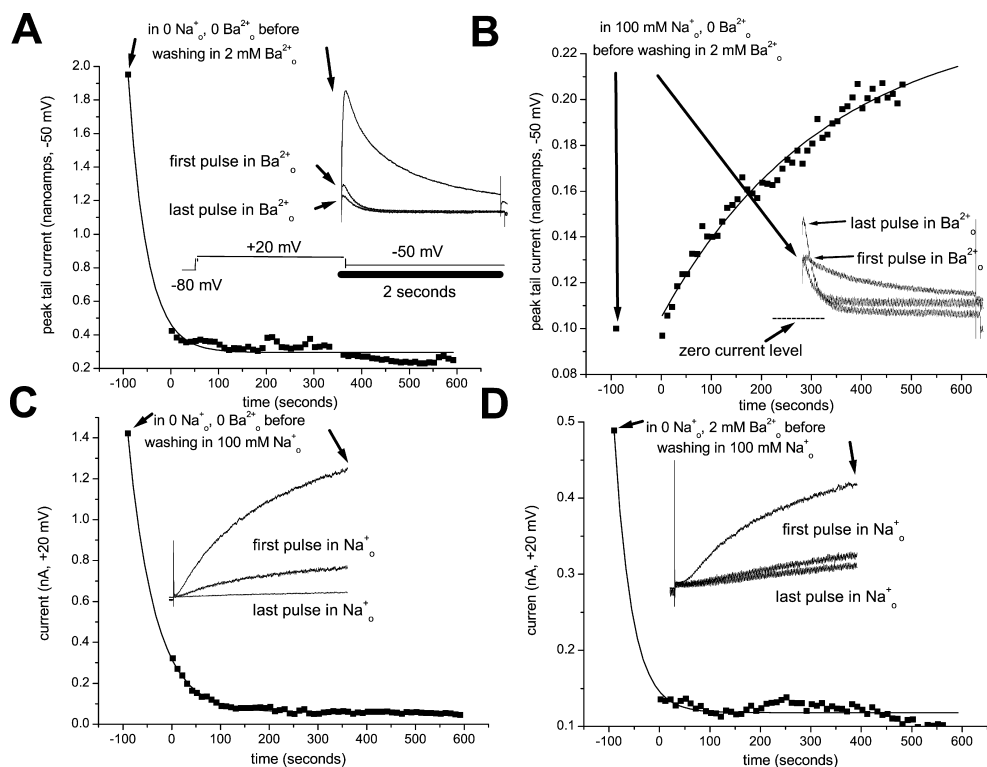
A in 0 Na^+_o, 0 Ba$^{2+}_o$ before washing in 2 mM Ba$^{2+}_o$
first pulse in Ba$^{2+}_o$
last pulse in Ba$^{2+}_o$
+20 mV
−50 mV
−80 mV
2 seconds
peak tail current (nanoamps, −50 mV)
time (seconds)

B in 100 mM Na^+_o, 0 Ba$^{2+}_o$ before washing in 2 mM Ba$^{2+}_o$
last pulse in Ba$^{2+}_o$
first pulse in Ba$^{2+}_o$
zero current level
peak tail current (nanoamps, −50 mV)
time (seconds)

C in 0 Na^+_o, 0 Ba$^{2+}_o$ before washing in 100 mM Na^+_o
first pulse in Na^+_o
last pulse in Na^+_o
current (nA, +20 mV)
time (seconds)

D in 0 Na^+_o, 2 mM Ba$^{2+}_o$ before washing in 100 mM Na^+_o
first pulse in Na^+_o
last pulse in Na^+_o
current (nA, +20 mV)
time (seconds)

FIGURE 9. Na^+_o slows onset of Ba$^{2+}_o$ effect, but Ba$^{2+}_o$ does not slow onset of Na$^+$ effect. Cells were held at −80 mV and stepped to 20 mV for 2 s followed by a 2-s step to −50 mV. Current was first recorded in one solution ($t = −90$ s), and the cell was then held at −80 while the solution was exchanged, adding either 100 mM Na^+_o or 2 mM Ba$^{2+}_o$. At $t = 0$, cells were repeatedly pulsed for 10 min. Representative cells for each of four solution permutations are shown in A–D. For each solution permutation, similar results were obtained in four different cells. (A) Adding Ba^{2+} without Na$^+$. (B) Adding Ba^{2+} with Na$^+$. (C) Adding Na$^+$ without Ba^{2+}. (D) Adding Na$^+$ with Ba^{2+}. For experiments in which Ba^{2+} was washed in, peak tail current was measured. For experiments in which Na$^+$ was washed in, current at the end of the 2-s depolarizing step was measured. Note that in B, current increased after Ba^{2+} was washed in, consistent with the relief of Na^+_o inhibition by Ba$^{2+}_o$ observed in Fig. 7. The time necessary for current level to equilibrate to new solution conditions was much greater for condition B.

that Ba$^{2+}_o$ unblock will be impaired in any inactivation-impaired mutant. We found this prediction to be fulfilled for S624A; sustained Ba$^{2+}_o$ block of this inactivation-impaired channel was greater than that observed in WT HERG (compare Figs. 8 C and 7 C, 2 mM Ba$^{2+}_o$). Further, in S624A, Ba$^{2+}_o$ and Na^+_o together yielded a degree of current inhibition greater than that seen with either cation alone (Fig. 8, A and C), unlike the relief of Na^+_o inhibition seen in WT (Fig. 8 C). That is, Ba^{2+} attenuation of Na^+_o inhibition was absent in the inactivation-impaired mutant S624A, consistent with the idea that strong relief of Ba$^{2+}_o$ block (due to intact inactivation) is of central importance to the attenuation phenomenon.

Given the decreased sensitivity of S624A to inhibition by Na^+_o, a model in which Na^+_o binds at an external site where it opposes Ba$^{2+}_o$ egress predicts a reduced effect of Na^+_o on Ba$^{2+}_o$ egress in S624A relative to WT HERG. That is, Na^+_o should evoke less slowing of the HERG current rise time in 2 mM Ba$^{2+}_o$ in the mutant compared with WT HERG. Interpretation of the S624A data is clouded by the fact that 100 mM Na^+_o in the absence of Ba$^{2+}_o$ increases the $t_{1/2}$ (Fig. 8, B and D), a phenomenon not observed for WT HERG. However, in contrast to WT (Fig. 7 D), adding 100 mM Na^+_o on top of 2 mM Ba$^{2+}_o$ increases the $t_{1/2}$ in a manner indistin-

guishable from adding 100 mM Na^+_o alone (Fig. 8 D, $\Delta t_{1/2} = 228 \pm 12$ ms vs. 252 ± 37 ms, respectively, P = 0.55). Thus, the $t_{1/2}$ data for S624A are also consistent with a model in which Na^+_o inhibits current at an external site where it opposes Ba$^{2+}_o$ egress.

Sodium Slows Onset of Barium Effect, but Barium Fails to Slow Onset of the Sodium Effect

The model described above postulates simultaneous occupancy of discrete sites for Na^+_o and Ba$^{2+}_o$, with Na$^+$ external to Ba^{2+}. The relief of Na^+_o inhibition of WT HERG by Ba$^{2+}_o$ (Fig. 7, A and C) could conceivably be explained by competition of the two cations for a common site. The lack of a predominant field effect in Na^+_o inhibition (Fig. 1) argues against a common site, but it is possible that a field effect could be masked by inactivation favoring Na^+_o inhibition (see earlier discussion of Fig. 1). The model with discrete sites predicts that Na^+_o should protect channels from the onset of Ba$^{2+}_o$ effects, whereas Ba$^{2+}_o$ should be relatively ineffective at protecting channels from Na^+_o. Fig. 9, A and B, show the results from representative experiments in which the time course of onset of Ba^{2+} effects was observed in the absence and presence of Na$^+$, respectively. Because Ba^{2+} block is most prominent at hyperpolarized potentials, peak tail currents were used to

FIGURE 10. WT HERG dose-response relationships for Na^+_o in presence of Ba^{2+}. Cells were stepped from a holding potential of -80 to 20 mV for 2 s, followed by a 2-s step to -50 mV. $[K^+]_o$ was held at 0 in these experiments. (A) Representative WT currents from a cell washed through consecutive solutions of varying $[Na^+]_o$ as shown. (B) Currents from A at 20 mV scaled to show the rate of current rise. Arrows indicate the $t_{1/2}$ (time to half-maximal current value). (C) For several cells as in A ($n = 4$–7), current at the end of the 2-s depolarizing step (A, arrows) was normalized to the value in 0 Na^+_o, 0 Ba^{2+}_o. The resulting dose-response relationship (C) is much less steep than the Na^+_o dose-response in the absence of Ba^{2+} (see Fig. 4E). (D) For several cells as in B ($n = 4$–7)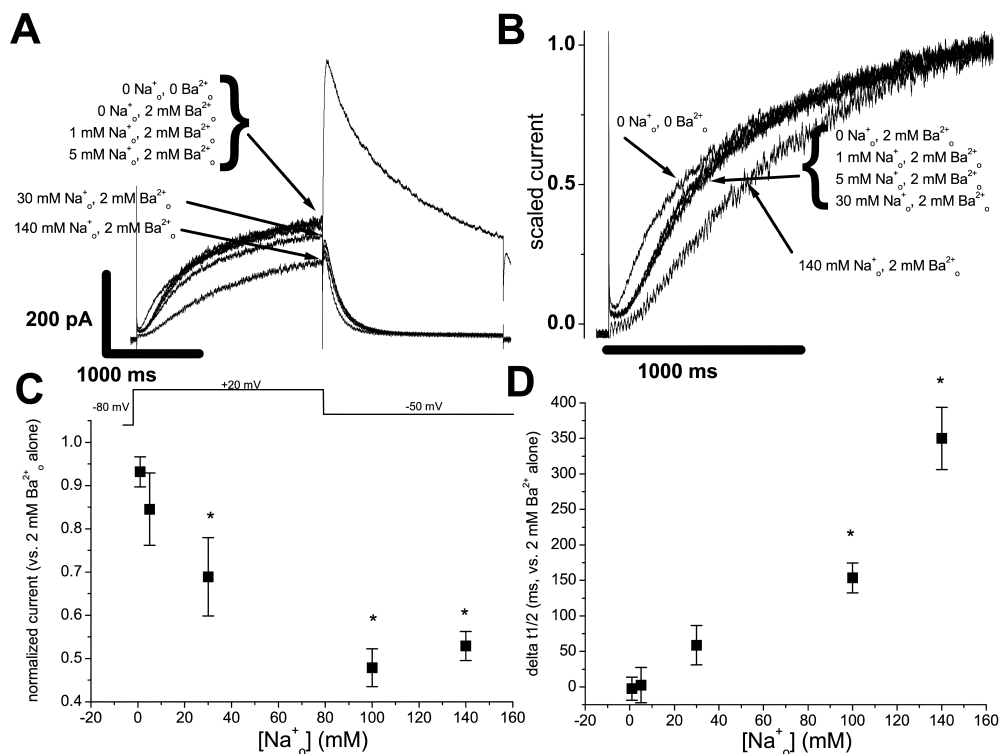, $\Delta t_{1/2}$ values were calculated by subtracting the $t_{1/2}$ in 0 Na^+_o, 2 mM Ba^{2+}_o from the $t_{1/2}$ in variable $[Na^+]_o$, 2 mM Ba^{2+}_o. More than 30 mM Na^+_o was required to increase the $t_{1/2}$ value (P for $\Delta t_{1/2}$ vs. 0 = 0.12 for 30 mM, P < 0.01 for 100 and 140 mM Na^+). Data at 100 mM Na^+ are taken from experiments like those shown in Fig. 7; summarized data at 100 mM are identical to those shown in Fig. 7.

quantify the time course for each cell. Cells were pre-equilibrated to 0 Na^+_o or 100 mM Na^+_o solutions before a 90-s period in which 2mM Ba^{2+} was washed in, and then pulsed repeatedly to 20 mV for 10 min. Upon exposure to Ba^{2+}, peak tail currents decreased in the absence of Na^+_o (Fig. 9 A) but increased in the presence of Na^+_o (Fig. 9 B), consistent with the previously described relief of Na^+_o inhibition by Ba^{2+}_o (Fig. 7, A and C). Currents were much slower to equilibrate to Ba^{2+}_o in the presence of Na^+_o (Fig. 9 B). In complementary experiments (Fig. 9, C and D), the time course of onset of Na^+_o effects was observed in the presence and absence of Ba^{2+}_o. Because Na^+_o effects in the presence of Ba^{2+}_o are most prominent at depolarized potentials, currents at the end of the 2-s depolarizing pulse were used to quantify the time course for each cell. Onset of Na^+_o effects occurred quickly both in the absence (Fig. 9 C) and the presence (Fig. 9 D) of Ba^{2+}_o. The results are consistent with a model of the HERG pore that includes two discrete sites, a more internal Ba^{2+} site and a more external site for Na^+_o.

Apparent Affinities of the HERG Outer Pore for Sodium and Potassium Differ by 30–50-fold

Neyton and Miller (1988b) first applied the method of monitoring Ba^{2+} off-rate to determine outer pore affin-ity of BK channels for K^+_o. Our studies of the Na^+_o interaction with HERG began with attempts to understand the anti-Nernstian effect of K^+_o and suggested that K^+_o acts to potently relieve inhibition of outward HERG K^+ current by Na^+_o (Numaguchi et al., 2000a). We performed dose-response experiments with Na^+_o (Fig. 10) and K^+_o (Fig. 11) in the presence of 2 mM Ba^{2+}_o to define the relative sensitivities of Ba^{2+} egress to the two cations. These sensitivities are most parsimoniously interpreted as relative affinities of Na^+_o and K^+_o for the HERG outer pore. Panels A and B of these figures show raw and scaled traces, respectively, while panels C and D summarize data with respect to current magnitude and $t_{1/2}$. 30 mM Na^+_o or more was required to significantly increase $t_{1/2}$ (Fig. 10 D). Current magnitude declined in parallel with increasing $t_{1/2}$ (Fig. 10 C). Lower $[K^+]_o$ was required to increase $t_{1/2}$ (Fig. 11 D). A large increase in $t_{1/2}$ was observed between 1 and 5 mM, which corresponds roughly to the physiologic range of serum K^+. In the absence of Ba^{2+}_o, 5 mM K^+_o caused only a modest increase in $t_{1/2}$ (54 $\pm$ 12 ms vs. 231 $\pm$ 12 ms for 5 mM K^+_o with 2 mM Ba^{2+}_o, P < 0.01), indicating that the K^+_o effect on $t_{1/2}$, like the Na^+_o effect (Fig. 7), reflects slowing of Ba^{2+}_o egress. Current magnitude was largely unaffected by $[K^+]_o$ in the presence of 2 mM Ba^{2+}_o (Fig. 11 C), despite the reduction in driving force as $[K^+]_o$ was raised.

A

100 uM K^+_o, 2 mM Ba$^{2+}_o$
1 mM K^+_o, 2 mM Ba$^{2+}_o$

0 K^+_o, 0 Ba$^{2+}_o$
0 K^+_o, 2 mM Ba$^{2+}_o$
20 uM K^+_o, 2 mM Ba$^{2+}_o$

200 pA

5 mM K^+_o, 2mM Ba$^{2+}_o$

1000 ms

B

scaled current

0 K^+_o, 0 Ba$^{2+}_o$

0 K^+_o, 2 mM Ba$^{2+}_o$
20 uM K^+_o, 2 mM Ba$^{2+}_o$
100 uM K^+_o, 2 mM Ba$^{2+}_o$
1 mM K^+_o, 2 mM Ba$^{2+}_o$

5 mM K^+_o, 2mM Ba$^{2+}_o$

C

+20 mV
−80 mV
−50 mV

normalized current (vs. 2 mM Ba$^{2+}_o$ alone)

[K^+_o] (mM)

D

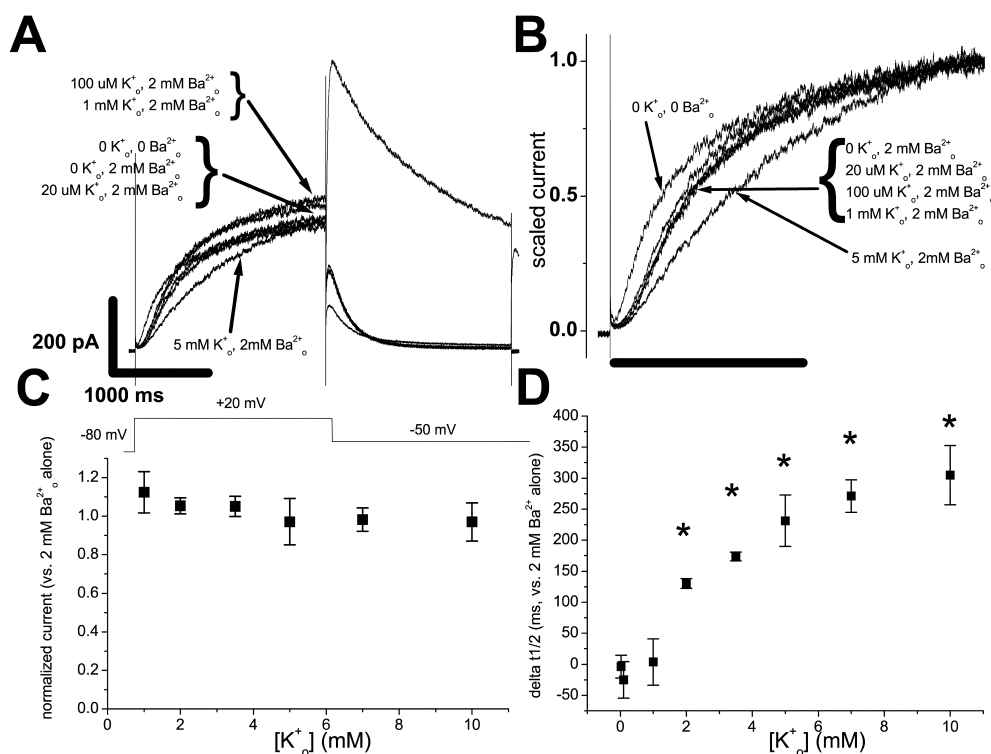delta t1/2 (ms, vs. 2 mM Ba$^{2+}_o$ alone)

[K^+_o] (mM)

FIGURE 11. WT HERG dose-response relationships for K^+_o in presence of Ba^{2+}. Cells were stepped from a holding potential of −80 to 20 mV for 2 s, followed by a 2-s step to −50 mV. [Na$^+$]$_o$ was held at 0 in these experiments. (A) Representative WT currents from a cell washed through consecutive solutions of varying [K$^+$]$_o$ as shown. (B) Currents from A at 20 mV scaled to show the rate of current rise. Arrows indicate the $t_{1/2}$ (time to half-maximal current value). (C) For several cells as in A ($n = 4$), current at the end of the 2-s depolarizing step (A, arrows) was normalized to the value in 0 K^+_o, 0 Ba$^{2+}_o$. The resulting dose-response relationship is less steep than the K^+_o dose-response in the absence of Ba^{2+} (compare with Fig. 6 C). Normalized current in 5 mM K^+_o, 0 Ba$^{2+}_o$ was significantly greater than normalized current with 5 mM K^+_o, 2 mM Ba$^{2+}_o$ (P < 0.01). (D) For several cells as in B ($n = 4$), $\Delta t_{1/2}$ values were calculated by subtracting the $t_{1/2}$ in 0 K^+_o, 2 mM Ba$^{2+}_o$ from the $t_{1/2}$ in variable [K$^+$]$_o$, 2 mM Ba$^{2+}_o$. More than 1 mM K^+_o was required to significantly increase the $t_{1/2}$ value (P for $\Delta t_{1/2}$ vs. 0 > 0.45 for K^+_o of 1 mM and lower, P < 0.02 for 2 mM K^+_o and higher).

The capacity for precise quantitative analysis of Ba^{2+} off-rates and site affinities for Na^+_o and K^+_o is limited by our making population measurements, by the relatively slow speed of HERG channel activation, and by the fact that a Ba^{2+} ion occupies the channel pore at a site near the Na^+_o/K^+_o site. Still, by assuming that equal fractional occupancy of an outer pore site leads to equal change in $t_{1/2}$ in the presence of Ba^{2+}, we can make an estimate of the relative site affinities. The effect of 100 mM Na^+_o ($\Delta t_{1/2} = 154 \pm 21$ ms) falls between those of 2 mM K^+_o (130 ± 8 ms) and 3.5 mM K^+_o (173 ± 7 ms). Overall, then, the data suggest a difference of 30–50-fold in the affinities of the HERG outer pore for the two cations.

Extended Time at the Holding Potential Promotes Current Inhibition by Extracellular Sodium in WT HERG, but not in the Mutant S624A

The localization of Na^+_o to the HERG outer pore (Figs. 7 and 9) and the low apparent K$^+$ affinity of the HERG outer pore (Fig. 11), together with our desire to understand the plateau in the Na^+_o dose-response curve for S624A and S624T (Fig. 4 E), prompted us to reconsider the role of the closed state in Na^+_o inhibition. To quickly deactivate channels after an activating pulse, we modified our pulse-train protocol to include only an activating pulse to 20 mV and the holding po-

tential of −80 mV (Fig. 12, inset). Steady-state block of WT current by 1 mM Na$^+$ at the end of 2-s steps to 20 mV was compared for several intervals at −80 mV (Fig. 12, A–C). Block was significantly greater for longer intervals (P < 0.05 for 2 s vs. each longer interval, Fig. 12 C) and the effect of closed time appears to be nearing saturation at 16 s. For experiments with S624A, 20 mM Na^+_o was used in order to start at a level of fractional block similar to that observed with 1 mM for the WT channel. In contrast to WT HERG, no effect of pulsing frequency on Na^+_o inhibition was observed for the mutant S624A (P > 0.18 for 2 s vs. each longer interval, Fig. 12, D–F). Models with the potential to explain these data are considered in the discussion section.

DISCUSSION

Sodium Permeation in Other Potassium Channels

Na^+_o can block inward rectifier (K$_{ir}$) channels (Owen et al., 1999), and has been shown to block Ca^{2+} influx through the ciliary P2X receptor (Ma et al., 1999). However, Na^+_o does not generally block voltage-gated K$^+$ channels (Hille, 2001). Intracellular Na$^+$ (Na^+_i) block of voltage-gated K$^+$ channels, by contrast, is well-described (Bezanilla and Armstrong, 1972; French and Wells, 1977; Yellen, 1984a,b; Pusch et al., 2001).

FIGURE 12. Effect of pulsing frequency on Na^+_o inhibition of WT HERG and S624A. Cells were stepped from a holding potential of -80 to 20 mV for 2 s, followed by an immediate step back to the holding potential of -80 mV. $[K^+]_o$ was held at 0 in these experiments. The interval at -80 mV was varied between 2 and 16 s. A and B show representative WT HERG cells recorded while pulsing with 4- and 8-s intervals at -80 mV, respectively. Cells were first recorded in 0 Na^+_o and subsequently in 1 mM Na^+_o. Current in 1 mM Na^+_o at the end of the 2 s depolarizing step (A and B, arrows) was normalized to the value in 0 Na^+_o. Data from several experiments ($n = 4$–6 for each interval) are summarized in C. For WT HERG, normalized current was significantly smaller for longer intervals at -80 mV (P < 0.05 for 2 s vs. each longer interval). D and E show representative S624A cells recorded while pulsing with 4- and 8-s intervals at -80 mV, respectively. Cells were first recorded in 0 Na^+_o and subsequently in 20 mM Na^+_o, to give a level of fractional block similar to that tested in WT (A–C). Current in 20 mM Na^+_o at the end of the 2-s depolarizing step (D and E, arrows) was normalized to the value in 0 Na^+_o. Data from several experiments ($n = 4$–6 for each interval) are summarized in F. For S624A, there was no significant difference in normalized current as the interval at -80 mV was increased (P > 0.18 for 2 s vs. each longer interval).
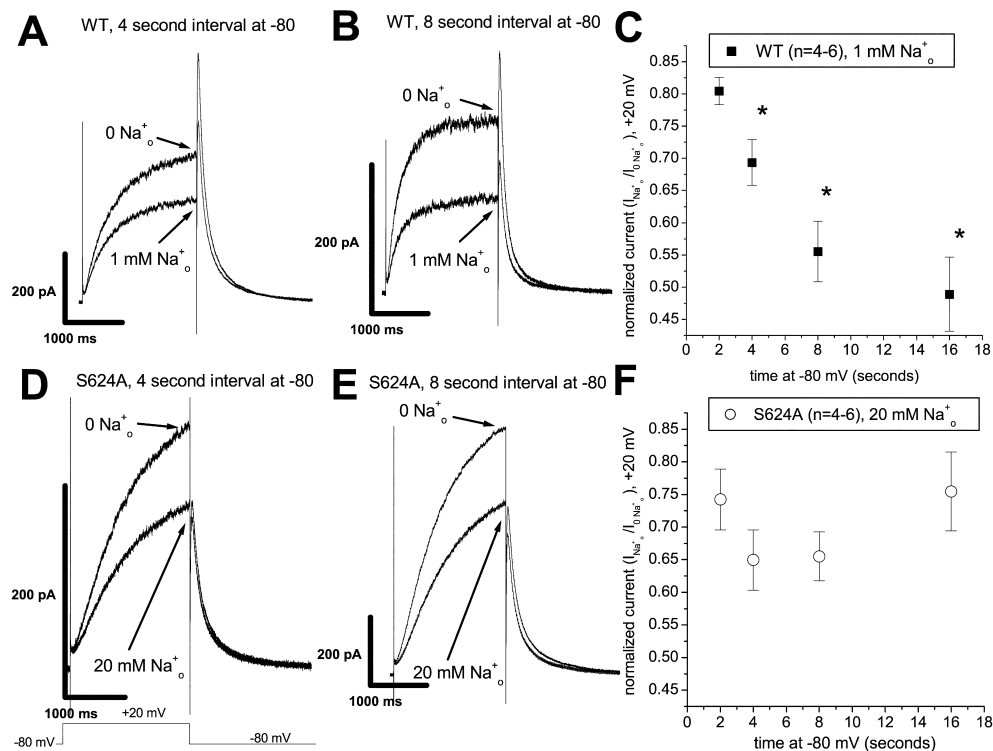
Indeed, sidedness of Na^+ block was one of the criteria used to determine the absolute orientation of the bacterial channel KcsA in lipid bilayers (Heginbotham et al., 1999) and the membrane topology of the K^+-selective prokaryotic glutamate receptor GluR0 (Chen et al., 1999). Still, several studies have shown that voltage-gated K^+ channels can interact with Na^+_o (Lopez-Barneo et al., 1993) and even allow Na^+ permeation in permissive (low K^+) conditions (Callahan and Korn, 1994; Korn and Ikeda, 1995; Starkus et al., 1997, 1998, 2000; Kiss et al., 1998, 1999; Ogielska and Aldrich, 1998, 1999; Wang et al., 2000a,b). Further, this Na^+ permeation is often most prominent in the C-type–inactivated state. Systematic variation of internal and external cation concentrations in Shaker has led to the following reinterpretation of the mechanism of C-type inactivation: C-type–inactivated channels are nonconducting in physiological conditions because a conformational change renders an outer pore site relatively Na^+ selective, whereas an inner site remains potently blocked by K^+ (Starkus et al., 1997, 1998). Shaker C-type inactivation lacks intrinsic voltage dependence in standard solution conditions (Hoshi et al., 1991), but intrinsic voltage dependence can appear under conditions of balanced competition between Na^+ and K^+. This apparent voltage dependence of inactivation may arise from the voltage-dependent changes in relative K^+ and Na^+ permeabilities now thought to define the C-type inactivation process (Starkus et al., 2000).

The P-loop region, which mediates ion selectivity (Heginbotham et al., 1994) and classical C-type inactivation (Liu et al., 1996) in K^+ channels, has also been implicated in HERG's rapid, voltage-dependent inactivation process (Schonherr and Heinemann, 1996; Smith et al., 1996; Herzberg et al., 1998; Zou et al., 1998; Fan et al., 1999). Therefore, the studies in Shaker suggested that a fruitful approach to understanding both Na^+_o effects on HERG and the HERG inactivation gating mechanism would be to lower or remove K^+ in the experimental system, record Na^+ currents through HERG channels, and interrogate the relationship between Na^+ permeation and inactivation gating. There is at least one published report of drug-induced Na^+ permeability of HERG channels in oocytes (Ulens et al., 1999). In our studies, conducted in CHO cells and in the absence of drugs, Na^+ currents through HERG could not be detected despite attempts with several internal/external solution combinations in WT and S624A (unpublished data).

Extracellular Sodium Interacts with the HERG Channel at an Outer Pore Site

In this study, Na^+_i and Ba^{2+}_o were used as probes to narrow the field of possible locations for Na^+_o interaction with the HERG channel. Observation of similar effects of Na^+_o and Na^+_i would implicate the channel pore. We found that physiologic $[Na^+]_i$ inhibited WT HERG current in a voltage-dependent manner similar to the inner cavity block described for other voltage-gated K^+ channels (Bezanilla and Armstrong, 1972; French and Wells, 1977; Yellen, 1984a,b; Pusch et al., 2001). Further, Na^+_i effects on WT and S624A HERG channels were similar, and the presence of Na^+_i did not affect Na^+_o inhibition in the WT channel. These results suggested that Na^+_o was unlikely to act by binding in the inner pore or by permeating the channel in an occult manner to reach the inner cavity. The results with Na^+_i did not directly address the question of whether Na^+_o acts by a remote allosteric mechanism or by occluding the outer pore.

Three HERG point mutants (S624A, S624T, S631A) with impaired inactivation had reduced sensitivity to inhibition by Na^+_o (Fig. 4). This result suggested that the HERG-inactivated state might be important to the mechanism by which Na^+_o inhibits current. There is precedent for an external cation (Ca^{2+}_o) to inhibit HERG current via an allosteric mechanism by binding to a site remote from the pore (Johnson et al., 1999, 2001). We used Ba^{2+}_o as a probe to distinguish between two simple models for Na^+_o inhibition of HERG current, remote allosteric stabilization of the inactivated state versus outer pore occlusion. Ba^{2+}_o block is relieved by HERG inactivation (Weerapura et al., 2000), a feature critical to the interpretation of our experiments combining Ba^{2+}_o and Na^+_o. A simple remote allosteric model in which Na^+_o stabilizes the HERG-inactivated state predicts that Na^+_o will speed Ba^{2+}_o egress from the channel. Instead, Na^+_o slowed Ba^{2+}_o egress from HERG as inferred from the rate of current rise (Fig. 7, B and D). Further, Ba^{2+}_o was found to relieve Na^+_o inhibition of HERG (Fig. 7, A and C), and Na^+_o was able to protect against onset of Ba^{2+}_o effects (Fig. 9). These data are most consistent with discrete sites for Na^+_o and Ba^{2+}_o in the outer and inner HERG pore, respectively. The data suggest that Ba^{2+} sweeps Na^+_o from the pore as it exits inactivated HERG channels (Fig. 7 B, cartoon).

Competition between Extracellular Sodium and Potassium for the HERG Channel Pore

Because K^+_o and Na^+_o interact with the HERG channel in a nonadditive manner (Numaguchi et al., 2000a), one attractive hypothesis is that the two cations compete for the HERG outer pore. Dose-response experi-

ments comparing the abilities of Na^+_o (Fig. 10) and K^+_o (Fig. 11) to slow Ba^{2+} egress from HERG supported the plausibility of such a model. K^+_o in the 2–10 mM range was sufficient to slow Ba^{2+} egress (Fig. 11 D), whereas Na^+_o in the 30–140 mM range was needed (Fig. 12 D). Although these experiments do not directly measure site affinity, the simplest interpretation of the data suggests an $\sim$30–50-fold greater affinity for K^+ than Na^+, values that would permit competition of physiological $[Na^+]_o$ and $[K^+]_o$ for an outer pore site.

The 30–50-fold difference in affinity contrasts markedly with the 1,000-fold difference in site affinity described by Neyton and Miller (1988b) for the BK channel (K_i = 19 μM for K^+_o, 27 mM for Na^+_o). Ignoring momentarily the many methodological divergences in our studies and the possibility of subtle differences in the position where Ba^{2+} resides in HERG versus BK channels, it would appear that the major difference between the HERG outer pore and the BK channel outer pore is not that HERG has a much greater affinity for Na^+, but instead that HERG has lower affinity for K^+. In other (non-HERG) K^+ channels, very high K^+ affinity could explain the inability of Na^+_o to inhibit current; in such cases, even closed channels could potentially retain permeating K^+, thereby preventing Na^+_o from binding. In the presence of K^+_o, the outer pore would be even more likely to be occupied by K^+, as it could enter from the extracellular side.

Rate Dependence of Inhibition by Extracellular Sodium in WT HERG, but not S624A

Our desire to understand the plateau in the Na^+_o dose-response curve for HERG S624A and S624T (Fig. 4 E) motivated us to more carefully study the role of the closed state in Na^+_o inhibition. For WT HERG, greater inhibition was observed with extended time at the holding potential of -80 mV (Fig. 12, A–C), whereas no such effect of holding potential was observed for S624A (Fig. 12, D–F). Earlier, we described a modest trend toward decreased Na^+_o inhibition at more hyperpolarized test potentials for WT HERG (Fig. 1 C). Therefore, the effect of time at -80 mV in WT HERG (Fig. 12 C) suggests a permissive role of the closed state in Na^+_o inhibition. The closed state of the S624A channel apparently does not permit additional Na^+_o inhibition (Fig. 12 F). Regardless of the underlying basis, the insensitivity of Na^+_o inhibition to closed time in S624A helps reconcile this mutant's unusual Na^+_o dose-response curve (Fig. 4 E). The insensitivity to closed time must, on some level, reflect a reduced affinity of Na^+_o for the S624A closed state as compared with WT. A lower closed state affinity could arise directly from a change in the structure of the channel protein resulting from the amino acid substitution. Alternatively, the insensitivity of S624A to time at -80 mV could be the indirect

FIGURE 13. A putative structural effect of mutations at the HERG S624 position. (A) Selectivity filter skeleton of KcsA (Doyle et al., 1998) color-coded and annotated to reflect the HERG sequence. Residue positions in red are identical in KcsA and HERG. Residue positions in green are nonidentical in KcsA and HERG. One such residue, KcsA Y82, which is positionally equivalent to HERG S631, is annotated on the figure. Shown in purple and also annotated is KcsA T75, positionally equivalent to HERG S624. Numbers superimposed on ion positions reflect the nomenclature applied in a recent crystallographic study of the KcsA channel (Morais-Cabral et al., 2001). (B) View of KcsA T75 from the bottom (inside) of the selectivity filter. Atomic detail is shown only for T75. A heavy atom distance criterion was applied to the KcsA structure to identify putative hydrogen bonds. A potential ring of hydrogen bonds encircling the inner selectivity filter and involving both inter- and intrasubunit interactions between T75 residues was identified (dotted white lines). This putative ring incorporates alternating interactions between backbone carbonyl and side chain hydroxyl moieties of T75. Heavy atom distances in putative bonds are all <3 Å. By analogy, if S624 residues were to exist in a similar structure in the HERG channel, then the S624A mutation would be expected to disrupt the hydrogen bond ring by eliminating side chain hydroxyl moieties. By altering selectivity filter site 4, this kind of change could conceivably favor a "1,3"-like K^+ configuration in mutant channels (see text).
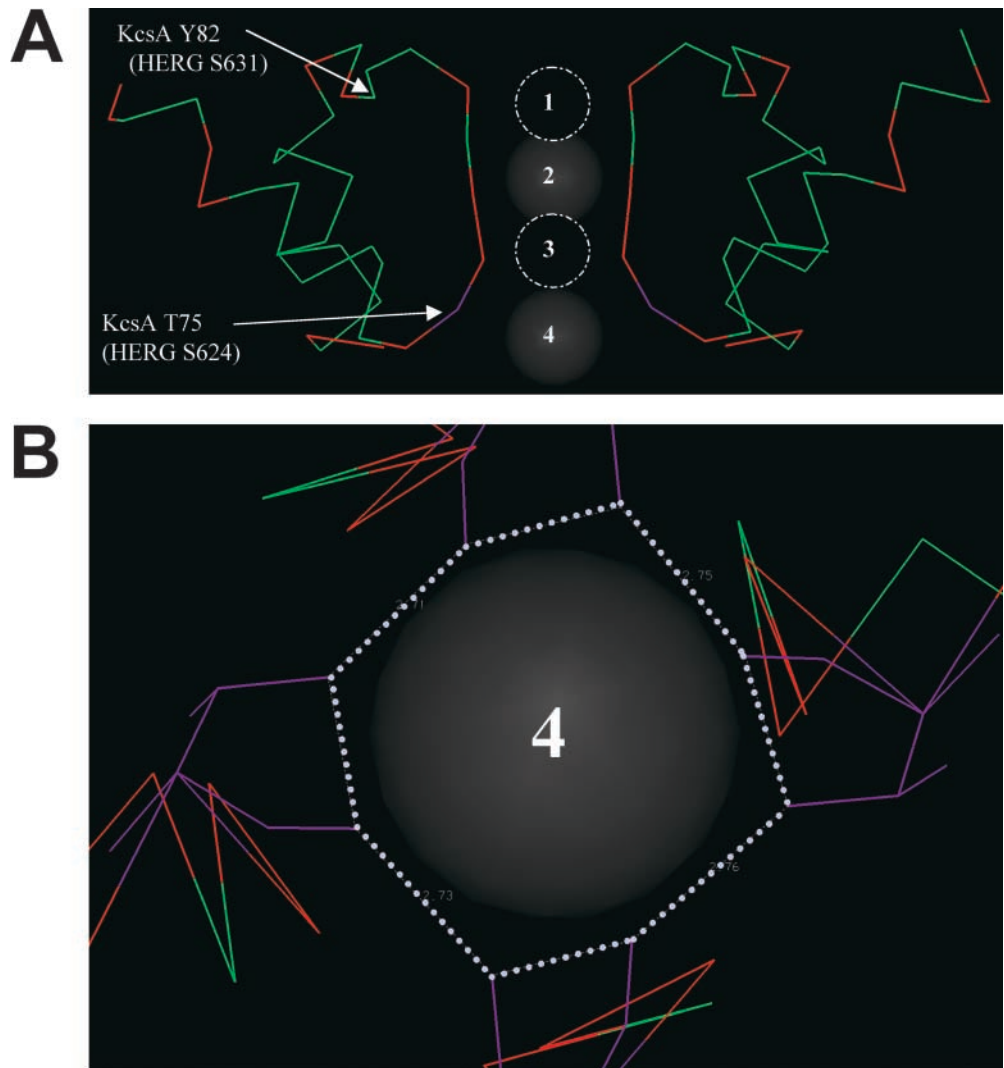
result of effects of the mutation on ion occupancy in the pore. This possibility is considered in some detail below, as it has the potential to explain several features of the phenotypes of mutants at the S624 position.

A Model that Combines Permeation and Gating

This section is speculative and focuses primarily on the mutant channels S624A and S624T. Inactivation of S631A is shifted by >100 mV (Zou et al., 1998), whereas the effects in the S624 mutations are much more modest (compare Fig. 4, A–D) and therefore more likely to reflect a pore structure similar to the WT HERG channel. Fig. 13 shows the predicted locations of HERG residues 631 and 624, using the crystal structure coordinates from the bacterial channel KcsA (Doyle et al., 1998). Serine 624 corresponds to the in-nermost selectivity filter position in KcsA (KcsA threonine 75). Application of a heavy atom distance criterion to locate putative hydrogen bonds within the KcsA structure identified a ring of predicted bonds between backbone carbonyl and side-chain hydroxyl moieties of threonine 75 encircling the inner selectivity filter (Fig. 13 B). By analogy with KcsA, the elimination of side chain hydroxyl moieties by the HERG S624A mutation would be expected to disrupt this putative ring of hydrogen bonds encircling the lower selectivity filter.

In the nomenclature of a recent crystallographic study of KcsA, the backbone carbonyl and side-chain hydroxyl moieties at KcsA T75 form "position 4," the in-nermost selectivity filter position (Morais-Cabral et al., 2001). In the model of permeation proposed by Morais-Cabral et al. (2001) independently supported by a

theoretical study (Berneche and Roux, 2001), K^+ and water occupy alternating positions in the selectivity filter such that two potassium ions occupy the filter simultaneously in configurations ("1,3" and "2,4") that are nearly energetically identical. Numbers corresponding to the terminology of Morais-Cabral et al. (2001) are superimposed on ions within the selectivity filter structures depicted in Fig. 13. Conceivably, the S624A and S624T mutations could decrease the energetic stability of the "2,4" state by altering the structure at position 4. Presumably this would favor the "1,3" configuration, thereby increasing the K^+ occupancy of the most outer pore site ("position 1"). Occupancy of such an outer pore site by K^+ is thought to slow C-type inactivation in Shaker-family channels (Lopez-Barneo et al., 1993; Baukrowitz and Yellen, 1995, 1996) and in HERG (Wang et al., 1996, 1997). Our experiments in this study support the conclusion that Na^+_o inhibits HERG current by binding to an outer pore site. Therefore, a phenomenon in which the "1,3" K^+ configuration is stabilized could conceivably underlie both the impaired inactivation of S624A and S624T (Fig. 3) and the mutants' decreased sensitivity to inhibition by Na^+_o (Fig. 4). The apparent saturation of Na^+_o inhibition for S624A and S624T at nonzero current levels (Fig. 4 E) could also be explained by such a scenario, in that a population of channels stabilized in the "1,3" K^+ configuration might be invulnerable to inhibition by Na^+_o.

Finally, channel closure at an intracellular activation gate (Liu et al., 1997; del Camino and Yellen, 2001; Tristani-Firouzi et al., 2002) would allow the selectivity filter to begin equilibrating with the low-$[K^+]_o$ external solution. Therefore, a stabilized "1,3" K^+ configuration could underlie the insensitivity of Na^+_o inhibition in S624A channels to extended time in the closed state (Fig. 12 F). For WT HERG, more frequent occupancy of the "2,4" K^+ configurations and/or loss of a K^+ ion to the external solution might provide a window of opportunity for Na^+_o to access the outer pore. Alternatively, equilibration of the pore with the external solution could promote a conformational change in the selectivity filter itself (Zhou et al., 2001) such that the pore might be more amenable to binding a Na^+ ion.

Comparison with Other Reports of Extracellular Sodium Inhibition of Potassium Currents

With regard to Na^+_o interactions with K^+ channels and the question of the potential uniqueness of the Na^+_o interaction with HERG, at least two additional groups of studies merit mention. First, Na^+_o block of inward K^+ currents carried by 3 mM K^+_o (Kiss et al., 1998) has been observed in a Kv1.3-Kv2.1 chimera. The IC_{50} for Na^+_o inhibition under these conditions was 100 mM, more than an order of magnitude higher than we ob-

serve for outward HERG current in high $[K^+]_i$ and 0 K^+_o. Notably, clear evidence of Na^+ permeation was seen in these studies, whereas we have been unable to resolve Na^+ currents in HERG. Interestingly, for this chimera, Na^+ currents and currents carried by very low $[K^+]$ inactivate in an intrinsically voltage-dependent manner. The authors consider the possibility that C-type inactivation has intrinsic voltage dependence and that fast, voltage-dependent events may normally be masked by saturation of the pore with K^+. According to this reasoning, the faster events are revealed only in conditions with lower pore occupancy (Kiss and Korn, 1998). Given our data suggesting a low K^+ affinity of the HERG outer pore (Fig. 7), a variant of this kind of limited occupancy hypothesis has the potential to help explain why HERG inactivation is voltage dependent in physiological K^+, even if the underlying basis of intrinsic voltage dependence remains elusive. Notably, recent fluorescence measurements have identified fast movements near the HERG S4 voltage sensor that may correlate with inactivation gating (Smith and Yellen, 2002).

Second, Na^+_o inhibition of delayed rectifier K^+ current in the bullfrog sympathetic ganglion has been reported under physiological conditions (Block and Jones, 1996, 1997). This effect was most prominent for inward currents recorded at very hyperpolarized potentials, whereas our experiments have defined a potent ability of Na^+_o to inhibit outward HERG current at depolarized potentials. As with the Kv1.3-Kv2.1 chimera, Na^+ can permeate the bullfrog K^+ channels. Further, the molecular identity of the channel studied in the bullfrog ganglion is unclear. That is, it is uncertain whether the relevant channel is more closely related to Shaker or ether-a-go-go family channels.

Implications for the Outer Pore of Ether-a-go-go Family Potassium Channels

Rat ether-a-go-go (r-eag) K^+ channels are blocked by Na^+_i (Pardo et al., 1998; Camacho et al., 2000). To our knowledge, no reports of Na^+_o effects on ether-a-go-go family K^+ channels other than HERG have been published. The question of whether channel inhibition by Na^+_o is specific to HERG or a general characteristic of ether-a-go-go family channels remains open, and suggests a potentially fruitful area of inquiry. Hydrogen bonding between the hydroxyl group of the tyrosine of the GYG signature sequence and consecutive tryptophan residues of the pore helix has been postulated to hold the KcsA selectivity filter open at the appropriate diameter to accommodate a K^+ ion (Doyle et al., 1998). HERG has a GFG selectivity filter sequence which is incompatible with this particular kind of hydrogen bonding. Fan et al. (1999) and Tseng (2001) have hypothesized that the GFG sequence may yield a relatively narrow and flexible outer pore structure

(Tseng, 2001), which may help explain both the fast kinetics of HERG inactivation (Fan et al., 1999) and the HERG channel's unusual susceptibility to inhibition by Na^+_o. The GFG sequence is neither sufficient to impart rapid voltage-dependent inactivation (Ganetzky et al., 1999; Ficker et al., 2001) nor necessary for it (Fleischhauer et al., 2000), but it seems likely to be important for voltage-dependent inactivation in HERG. The ability of Na^+_o to occupy the HERG outer pore as demonstrated in this study does not exclude the possibility that Na^+_o preferentially interacts with the HERG inactivated state. If HERG inactivation involves an outer pore constriction similar to classical C-type inactivation (Liu et al., 1996), then inactivated HERG channels might have high affinity for Na^+_o in accordance with the "close fit" hypothesis for ion selectivity (Mullins, 1959a,b; Starkus et al., 1997; Armstrong, 1998; Kiss et al., 1999). Interestingly, the initial characterization of a K^+ channel from the chlorella virus PBCV-1, which has a GFG selectivity filter sequence, was consistent with Na^+_o inhibition of outward K^+ current (Plugge et al., 2000).

Another region potentially important to HERG's pore properties is the channel's unusually long S5-P linker. Mutations in this linker can affect K^+/Na^+ selectivity and HERG inactivation gating (Dun et al., 1999), as well as binding of a HERG-specific scorpion peptide toxin (ErgTx) (Pardo-Lopez et al., 2002). These effects have prompted the proposal that the S5-P linker interacts closely with the HERG pore.

Physiological Implications of Sodium Effects on HERG Currents

Bradycardia is a recognized risk factor for QT prolongation and *torsades de pointes* (Roden, 1998). Much of the risk associated with bradycardia likely arises from marked depression of I_{KS} resulting from complete deactivation during increased time spent at hyperpolarized potentials. In the study defining the rate-dependence of I_{Ks}, performed in guinea pig myocytes, Jurkiewicz and Sanguinetti (1993) reported that the magnitude of I_{Kr} was rate independent. Interestingly, their measurements of I_{Kr} were made in the absence of Na^+_o. Our data showing rate dependence of Na^+_o inhibition of WT HERG current (Fig. 12, A–C) raise the possibility that the magnitude of I_{Kr} may be rate dependent in the presence of Na^+_o, and that this mechanism could underlie part of the *torsades* risk in bradycardic patients.

Physiologic $[Na^+]_i$ blocks HERG current at depolarized potentials (Fig. 5) and block is relieved by physiologic $[K^+]_o$ (Fig. 6). This suggests that the anti-Nernstian effect of $[K^+]_o$ on I_{Kr} in vivo is likely to reflect not only relief of inhibition by Na^+_o, but also relief of Na^+_i block. Further, $[Na^+]_i$ in beating cells may be higher

than usually thought (Wellis et al., 1990), raising the possibility that Na^+_i block of I_{Kr} and relief of that block by K^+_o could assume greater importance in vivo. It is also conceivable that K^+_o relief of Na^+_i block of cardiac K^+ channels other than HERG could contribute to the salutary effect of raising serum $[K^+]$ to normalize QT interval (Compton et al., 1996; Choy et al., 1997). Although the physiological relevance of Na^+_i block in other K^+ channels has remained somewhat unclear (Yellen, 1984b), a functional role for block of HERG by Na^+_i can be rationalized in a satisfying way. Voltage-dependent block by Na^+_i would be expected to preferentially limit HERG current in the early phases of the cardiac action potential when the membrane is strongly depolarized, and to be relieved in phase III, as I_{Kr} carries out its function of promoting rapid repolarization.

REFERENCES

Armstrong, C. 1998. The vision of the pore. *Science.* 280:56–57.

Armstrong, C.M., R.P. Swenson, Jr., and S.R. Taylor. 1982. Block of squid axon K channels by internally and externally applied barium ions. *J. Gen. Physiol.* 80:663–682.

Armstrong, C.M., and S.R. Taylor. 1980. Interaction of barium ions with potassium channels in squid giant axons. *Biophys. J.* 30:473–488.

Balser, J.R., P.B. Bennett, and D.M. Roden. 1990. Time-dependent outward current in guinea pig ventricular myocytes. Gating kinetics of the delayed rectifier. *J. Gen. Physiol.* 96:835–863.

Basso, C., P. Labarca, E. Stefani, O. Alvarez, and R. Latorre. 1998. Pore accessibility during C-type inactivation in Shaker K+ channels. *FEBS Lett.* 429:375–380.

Baukrowitz, T., and G. Yellen. 1995. Modulation of K+ current by frequency and external [K+]: a tale of two inactivation mechanisms. *Neuron.* 15:951–960.

Baukrowitz, T., and G. Yellen. 1996. Use-dependent blockers and exit rate of the last ion from the multi-ion pore of a K+ channel. *Science.* 271:653–656.

Berneche, S., and B. Roux. 2001. Energetics of ion conduction through the K+ channel. *Nature.* 414:73–77.

Bezanilla, F., and C.M. Armstrong. 1972. Negative conductance caused by entry of sodium and cesium ions into the potassium channels of squid axons. *J. Gen. Physiol.* 60:588–608.

Block, B.M., and S.W. Jones. 1996. Ion permeation and block of

M-type and delayed rectifier potassium channels. Whole-cell recordings from bullfrog sympathetic neurons. *J. Gen. Physiol.* 107: 473–488.

Block, B.M., and S.W. Jones. 1997. Delayed rectifier current of bullfrog sympathetic neurons: ion-ion competition, asymmetrical block and effects of ions on gating. *J. Physiol.* 499:403–416.

Callahan, M.J., and S.J. Korn. 1994. Permeation of Na+ through a delayed rectifier K+ channel in chick dorsal root ganglion neurons. *J. Gen. Physiol.* 104:747–771.

Camacho, J., A. Sanchez, W. Stuhmer, and L.A. Pardo. 2000. Cytoskeletal interactions determine the electrophysiological properties of human EAG potassium channels. *Pflugers Arch.* 441:167–174.

Chen, G.Q., C. Cui, M.L. Mayer, and E. Gouaux. 1999. Functional characterization of a potassium-selective prokaryotic glutamate receptor. *Nature.* 402:817–821.

Choy, A.M., C.C. Lang, D.M. Chomsky, G.H. Rayos, J.R. Wilson, and D.M. Roden. 1997. Normalization of acquired QT prolongation in humans by intravenous potassium. *Circulation.* 96:2149–2154.

Compton, S.J., R.L. Lux, M.R. Ramsey, K.R. Strelich, M.C. Sanguinetti, L.S. Green, M.T. Keating, and J.W. Mason. 1996. Genetically defined therapy of inherited long-QT syndrome. Correction of abnormal repolarization by potassium. *Circulation.* 94:1018–1022.

Curran, M.E., I. Splawski, K.W. Timothy, G.M. Vincent, E.D. Green, and M.T. Keating. 1995. A molecular basis for cardiac arrhythmia: HERG mutations cause long QT syndrome. *Cell.* 80:795–803.

del Camino, D., and G. Yellen. 2001. Tight steric closure at the intracellular activation gate of a voltage-gated k(+) channel. *Neuron.* 32:649–656.

Doyle, D.A., J. Morais Cabral, R.A. Pfuetzner, A. Kuo, J.M. Gulbis, S.L. Cohen, B.T. Chait, and R. MacKinnon. 1998. The structure of the potassium channel: molecular basis of K+ conduction and selectivity. *Science* 280:69–77.

Dun, W., M. Jiang, and G.N. Tseng. 1999. Allosteric effects of mutations in the extracellular S5-P loop on the gating and ion permeation properties of the hERG potassium channel. *Pflugers Arch.* 439:141–149.

Fan, J.S., M. Jiang, W. Dun, T.V. McDonald, and G.N. Tseng. 1999. Effects of outer mouth mutations on hERG channel function: a comparison with similar mutations in the Shaker channel. *Biophys. J.* 76:3128–3140.

Ficker, E., W. Jarolimek, and A.M. Brown. 2001. Molecular determinants of inactivation and dofetilide block in ether a-go-go (EAG) channels and EAG-related K(+) channels. *Mol. Pharmacol.* 60: 1343–1348.

Fleischhauer, R., M.W. Davis, I. Dzhura, A. Neely, L. Avery, and R.H. Joho. 2000. Ultrafast inactivation causes inward rectification in a voltage-gated K(+) channel from *Caenorhabditis elegans. J. Neurosci.* 20:511–520.

French, R.J., and J.B. Wells. 1977. Sodium ions as blocking agents and charge carriers in the potassium channel of the squid giant axon. *J. Gen. Physiol.* 70:707–724.

Ganetzky, B., G.A. Robertson, G.F. Wilson, M.C. Trudeau, and S.A. Titus. 1999. The eag family of K+ channels in *Drosophila* and mammals. *Ann. NY Acad. Sci.* 868:356–369.

Gomez-Lagunas, F. 1997. Shaker B K+ conductance in Na+ solutions lacking K+ ions: a remarkably stable non-conducting state produced by membrane depolarizations. *J. Physiol.* 499:3–15.

Gomez-Lagunas, F., and C.M. Armstrong. 1994. The relation between ion permeation and recovery from inactivation of ShakerB K+ channels. *Biophys. J.* 67:1806–1815.

Hamill, O.P., A. Marty, E. Neher, B. Sakmann, and F.J. Sigworth. 1981. Improved patch-clamp techniques for high-resolution current recording from cells and cell-free membrane patches. *Pflugers Arch.* 391:85–100.

Harris, R.E., H.P. Larsson, and E.Y. Isacoff. 1998. A permanent ion binding site located between two gates of the Shaker K+ channel. *Biophys. J.* 74:1808–1820.

Heginbotham, L., M. LeMasurier, L. Kolmakova-Partensky, and C. Miller. 1999. Single streptomyces lividans K(+) channels. Functional asymmetries and sidedness of proton activation. *J. Gen. Physiol.* 114:551–560.

Heginbotham, L., Z. Lu, T. Abramson, and R. MacKinnon. 1994. Mutations in the K+ channel signature sequence. *Biophys. J.* 66: 1061–1067.

Herzberg, I.M., M.C. Trudeau, and G.A. Robertson. 1998. Transfer of rapid inactivation and sensitivity to the class III antiarrhythmic drug E-4031 from HERG to M-eag channels. *J. Physiol.* 511:3–14.

Hille, B. 2001. Ion Channels of Excitable Membranes. 3rd Sinauer. Sunderland, MA. 814 pp.

Ho, W.K., I. Kim, C.O. Lee, J.B. Youm, S.H. Lee, and Y.E. Earm. 1999. Blockade of HERG channels expressed in *Xenopus* laevis oocytes by external divalent cations. *Biophys. J.* 76:1959–1971.

Hoshi, T., W.N. Zagotta, and R.W. Aldrich. 1991. Two types of inactivation in Shaker K+ channels: effects of alterations in the carboxy-terminal region. *Neuron.* 7:547–556.

Hurst, R.S., R. Latorre, L. Toro, and E. Stefani. 1995. External barium block of Shaker potassium channels: evidence for two binding sites. *J. Gen. Physiol.* 106:1069–1087.

Jiang, Y., and R. MacKinnon. 2000. The barium site in a potassium channel by X-ray crystallography. *J. Gen. Physiol.* 115:269–272.

Johns, D.C., H.B. Nuss, and E. Marban. 1997. Suppression of neuronal and cardiac transient outward currents by viral gene transfer of dominant-negative Kv4.2 constructs. *J. Biol. Chem.* 272: 31598–31603.

Johnson, J., F.M. Mullins, and P.B. Bennett. 1999. Human ether-a-go-go-related gene K+ channel gating probed with extracellular ca2+. Evidence for two distinct voltage sensors. *J. Gen. Physiol.* 113:565–580.

Johnson, J.P., Jr., J.R. Balser, and P.B. Bennett. 2001. A novel extracellular calcium sensing mechanism in voltage-gated potassium ion channels. *J. Neurosci.* 21:4143–4153.

Jurkiewicz, N.K., and M.C. Sanguinetti. 1993. Rate-dependent prolongation of cardiac action potentials by a methanesulfonanilide class III antiarrhythmic agent. Specific block of rapidly activating delayed rectifier K+ current by dofetilide. *Circ. Res.* 72:75–83.

Kiehn, J., A.E. Lacerda, and A.M. Brown. 1999. Pathways of HERG inactivation. *Am. J. Physiol.* 277:H199–210.

Kiehn, J., A.E. Lacerda, B. Wible, and A.M. Brown. 1996. Molecular physiology and pharmacology of HERG. Single-channel currents and block by dofetilide. *Circulation.* 94:2572–2579.

Kiss, L., D. Immke, J. LoTurco, and S.J. Korn. 1998. The interaction of Na+ and K+ in voltage-gated potassium channels. Evidence for cation binding sites of different affinity. *J. Gen. Physiol.* 111: 195–206.

Kiss, L., and S.J. Korn. 1998. Modulation of C-type inactivation by K+ at the potassium channel selectivity filter. *Biophys. J.* 74:1840–1849.

Kiss, L., J. LoTurco, and S.J. Korn. 1999. Contribution of the selectivity filter to inactivation in potassium channels. *Biophys. J.* 76: 253–263.

Korn, S.J., and S.R. Ikeda. 1995. Permeation selectivity by competition in a delayed rectifier potassium channel. *Science.* 269:410–412.

Liu, Y., M. Holmgren, M.E. Jurman, and G. Yellen. 1997. Gated access to the pore of a voltage-dependent K+ channel. *Neuron.* 19: 175–184.

Liu, Y., M.E. Jurman, and G. Yellen. 1996. Dynamic rearrangement

of the outer mouth of a K+ channel during gating. *Neuron.* 16: 859–867.

Lopez-Barneo, J., T. Hoshi, S.H. Heinemann, and R.W. Aldrich. 1993. Effects of external cations and mutations in the pore region on C-type inactivation of Shaker potassium channels. *Receptors Channels.* 1:61–71.

Ma, W., A. Korngreen, N. Uzlaner, Z. Priel, and S.D. Silberberg. 1999. Extracellular sodium regulates airway ciliary motility by inhibiting a P2X receptor. *Nature.* 400:894–897.

Miller, C. 1987. Trapping single ions inside single ion channels. *Biophys. J.* 52:123–126.

Miller, C., R. Latorre, and I. Reisin. 1987. Coupling of voltage-dependent gating and Ba++ block in the high-conductance, Ca++-activated K+ channel. *J. Gen. Physiol.* 90:427–449.

Mitcheson, J.S., J. Chen, M. Lin, C. Culberson, and M.C. Sanguinetti. 2000a. A structural basis for drug-induced long QT syndrome. *Proc. Natl. Acad. Sci. USA.* 94:12329–12333.

Monahan, B.P., C.L. Ferguson, E.S. Killeavy, B.K. Lloyd, J. Troy, and L.R. Cantilena, Jr. 1990. Torsades de pointes occurring in association with terfenadine use. *JAMA.* 264:2788–2790.

Morais-Cabral, J.H., Y. Zhou, and R. MacKinnon. 2001. Energetic optimization of ion conduction rate by the K+ selectivity filter. *Nature.* 414:37–42.

Mullins, F.M., R.R. Desai, A.L. George, Jr., and J.R. Balser. 2001. Two distinct effects of Na^+_o on HERG K^+ currents. *Biophys. J.* 80:216A.

Mullins, F.M., S.Z. Stepanovic, and J.R. Balser. 2002. Functional interaction between Na^+, K^+, and inactivation gating in the HERG pore. *Biophys. J.* 82:579a.

Mullins, L.J. 1959a. An analysis of conductance changes in the squid axon. *J. Gen. Physiol.* 42:1013–1035.

Mullins, L.J. 1959b. The penetration of some cations into muscle. *J. Gen. Physiol.* 42:817–829.

Neyton, J., and C. Miller. 1988a. Discrete Ba2+ block as a probe of ion occupancy and pore structure in the high-conductance Ca2+ -activated K+ channel. *J. Gen. Physiol.* 92:569–586.

Neyton, J., and C. Miller. 1988b. Potassium blocks barium permeation through a calcium-activated potassium channel. *J. Gen. Physiol.* 92:549–567.

Numaguchi, H., J.P. Johnson, Jr., C.I. Petersen, and J.R. Balser. 2000a. A sensitive mechanism for cation modulation of potassium current. *Nat. Neurosci.* 3:429–430.

Numaguchi, H., F.M. Mullins, J.P. Johnson, Jr., D.C. Johns, S.S. Po, I.C. Yang, G.F. Tomaselli, and J.R. Balser. 2000b. Probing the interaction between inactivation gating and Dd-sotalol block of HERG. *Circ. Res.* 87:1012–1018.

Ogielska, E.M., and R.W. Aldrich. 1998. A mutation in S6 of Shaker potassium channels decreases the K+ affinity of an ion binding site revealing ion-ion interactions in the pore. *J. Gen. Physiol.* 112: 243–257.

Ogielska, E.M., and R.W. Aldrich. 1999. Functional consequences of a decreased potassium affinity in a potassium channel pore. Ion interactions and C-type inactivation. *J. Gen. Physiol.* 113:347–358.

Owen, J.M., C.C. Quinn, R. Leach, J.B. Findlay, and M.R. Boyett. 1999. Effect of extracellular cations on the inward rectifying K+ channels Kir2.1 and Kir3.1/Kir3.4. *Exp. Physiol.* 84:471–488.

Pardo, L.A., A. Bruggemann, J. Camacho, and W. Stuhmer. 1998. Cell cycle-related changes in the conducting properties of r-eag K+ channels. *J. Cell Biol.* 143:767–775.

Pardo-Lopez, L., M. Zhang, J. Liu, M. Jiang, L.D. Possani, and G.N. Tseng. 2002. Mapping the binding site of a HERG-specific peptide toxin (ErgTx) to the channel's outer vestibule. *J. Biol. Chem.* 25:25.

Plugge, B., S. Gazzarrini, M. Nelson, R. Cerana, J.L. Van Etten, C.

Derst, D. DiFrancesco, A. Moroni, and G. Thiel. 2000. A potassium channel protein encoded by chlorella virus PBCV-1. *Science.* 287:1641–1644.

Pusch, M., L. Ferrera, and T. Friedrich. 2001. Two open states and rate-limiting gating steps revealed by intracellular Na+ block of human KCNQ1 and KCNQ1/KCNE1 K+ channels. *J. Physiol.* 533:135–143.

Rampe, D., M.L. Roy, A. Dennis, and A.M. Brown. 1997. A mechanism for the proarrhythmic effects of cisapride (Propulsid): high affinity blockade of the human cardiac potassium channel HERG. *FEBS Lett.* 417:28–32.

Roden, D.M. 1998. Taking the "idio" out of "idiosyncratic": predicting torsades de pointes. *Pacing Clin. Electrophysiol.* 21:1029–1034.

Roden, D.M., and J.R. Balser. 1999. A plethora of mechanisms in the HERG-related long QT syndrome. Genetics meets electrophysiology. *Cardiovasc. Res.* 44:242–246.

Roy, M., R. Dumaine, and A.M. Brown. 1996. HERG, a primary human ventricular target of the nonsedating antihistamine terfenadine. *Circulation.* 94:817–823.

Sanguinetti, M.C., C. Jiang, M.E. Curran, and M.T. Keating. 1995. A mechanistic link between an inherited and an acquired cardiac arrhythmia: HERG encodes the IKr potassium channel. *Cell.* 81: 299–307.

Sanguinetti, M.C., and N.K. Jurkiewicz. 1990. Two components of cardiac delayed rectifier K+ current. Differential sensitivity to block by class III antiarrhythmic agents. *J. Gen. Physiol.* 96:195–215.

Sanguinetti, M.C., and N.K. Jurkiewicz. 1992. Role of external Ca2+ and K+ in gating of cardiac delayed rectifier K+ currents. *Pflugers Arch.* 420:180–186.

Scamps, F., and E. Carmeliet. 1989. Delayed K+ current and external K+ in single cardiac Purkinje cells. *Am. J. Physiol.* 257:C1086–C1092.

Schonherr, R., and S.H. Heinemann. 1996. Molecular determinants for activation and inactivation of HERG, a human inward rectifier potassium channel. *J. Physiol.* 493:635–642.

Smith, P.L., T. Baukrowitz, and G. Yellen. 1996. The inward rectification mechanism of the HERG cardiac potassium channel. *Nature.* 379:833–836.

Smith, P.L., and G. Yellen. 2002. Fast and slow voltage sensor movements in HERG potassium channels. *J. Gen. Physiol.* 119:275–293.

Spector, P.S., M.E. Curran, A. Zou, M.T. Keating, and M.C. Sanguinetti. 1996. Fast inactivation causes rectification of the IKr channel. *J. Gen. Physiol.* 107:611–619.

Starkus, J.G., S.H. Heinemann, and M.D. Rayner. 2000. Voltage dependence of slow inactivation in Shaker potassium channels results from changes in relative K(+) and Na(+) permeabilities. *J. Gen. Physiol.* 115:107–122.

Starkus, J.G., L. Kuschel, M.D. Rayner, and S.H. Heinemann. 1997. Ion conduction through C-type inactivated Shaker channels. *J. Gen. Physiol.* 110:539–550.

Starkus, J.G., L. Kuschel, M.D. Rayner, and S.H. Heinemann. 1998. Macroscopic Na+ currents in the "Nonconducting" Shaker potassium channel mutant W434F. *J. Gen. Physiol.* 112:85–93.

Tao, B.Y., and K.C.P. Lee. 1994. Mutagenesis by PCR. *In* PCR Technology: Current Innovations. H.G. Griffin and A.M. Griffin, editors. CRC Press, London. 69–84.

Tristani-Firouzi, M., J. Chen, and M.C. Sanguinetti. 2002. Interactions between the S4-S5 linker and the S6 transmembrane domain modulate gating of HERG K+ channels. *J. Biol. Chem.* 25: 25.

Tseng, G.N. 2001. I(Kr): the hERG channel. *J. Mol. Cell. Cardiol.* 33: 835–849.

Ulens, C., P. Daenens, and J. Tytgat. 1999. Norpropoxyphene-induced cardiotoxicity is associated with changes in ion-selectiv-

ity and gating of HERG currents. *Cardiovasc. Res.* 44:568–578.

Wang, S., S. Liu, M.J. Morales, H.C. Strauss, and R.L. Rasmusson. 1997. A quantitative analysis of the activation and inactivation kinetics of HERG expressed in *Xenopus* oocytes. *J. Physiol.* 502:45–60.

Wang, S., M.J. Morales, S. Liu, H.C. Strauss, and R.L. Rasmusson. 1996. Time, voltage and ionic concentration dependence of rectification of h- erg expressed in *Xenopus* oocytes. *FEBS Lett.* 389: 167–173.

Wang, Z., J.C. Hesketh, and D. Fedida. 2000a. A high-Na(+) conduction state during recovery from inactivation in the K(+) channel kv1.5. *Biophys. J.* 79:2416–2433.

Wang, Z., X. Zhang, and D. Fedida. 2000b. Regulation of transient Na+ conductance by intra- and extracellular K+ in the human delayed rectifier K+ channel Kv1.5. *J. Physiol.* 523:575–591.

Weerapura, M., S. Nattel, M. Courtemanche, D. Doern, N. Ethier, and T. Hebert. 2000. State-dependent barium block of wild-type and inactivation-deficient HERG channels in *Xenopus* oocytes. *J. Physiol.* 526:265–278.

Wellis, D.P., L.J. DeFelice, and M. Mazzanti. 1990. Outward sodium current in beating heart cells. *Biophys. J.* 57:41–48.

Yang, T., D.J. Snyders, and D.M. Roden. 1997. Rapid inactivation determines the rectification and [K+]o dependence of the rapid component of the delayed rectifier K+ current in cardiac cells. *Circ. Res.* 80:782–789.

Yellen, G. 1984a. Ionic permeation and blockade in Ca2+-activated K+ channels of bovine chromaffin cells. *J. Gen. Physiol.* 84:157–186.

Yellen, G. 1984b. Relief of Na+ block of Ca2+-activated K+ channels by external cations. *J. Gen. Physiol.* 84:187–199.

Zhou, Y., J.H. Morais-Cabral, A. Kaufman, and R. MacKinnon. 2001. Chemistry of ion coordination and hydration revealed by a K+ channel-Fab complex at 2.0 A resolution. *Nature.* 414:43–48.

Zou, A., M.E. Curran, M.T. Keating, and M.C. Sanguinetti. 1997. Single HERG delayed rectifier K+ channels expressed in *Xenopus* oocytes. *Am. J. Physiol.* 272:H1309–H1314.

Zou, A., Q.P. Xu, and M.C. Sanguinetti. 1998. A mutation in the pore region of HERG K+ channels expressed in *Xenopus* oocytes reduces rectification by shifting the voltage dependence of inactivation. *J. Physiol.* 509:129–137.